

# Vascularized Bone Tissue Engineering: Approaches for Potential Improvement

Lonnissa H. Nguyen, Ph.D.,<sup>1,2,\*</sup> Nasim Annabi, Ph.D.,<sup>1,2,\*</sup> Mehdi Nikkhah, Ph.D.,<sup>1,2</sup>  
Hojae Bae, Ph.D.,<sup>1,2,†</sup> Loïc Binan, Ph.D.,<sup>3</sup> Sangwon Park, Ph.D.,<sup>4</sup> Yunqing Kang, Ph.D.,<sup>5</sup>  
Yunzhi Yang, Ph.D.,<sup>5</sup> and Ali Khademhosseini, Ph.D.<sup>1,2,6,7</sup>

Significant advances have been made in bone tissue engineering (TE) in the past decade. However, classical bone TE strategies have been hampered mainly due to the lack of vascularization within the engineered bone constructs, resulting in poor implant survival and integration. In an effort toward clinical success of engineered constructs, new TE concepts have arisen to develop bone substitutes that potentially mimic native bone tissue structure and function. Large tissue replacements have failed in the past due to the slow penetration of the host vasculature, leading to necrosis at the central region of the engineered tissues. For this reason, multiple microscale strategies have been developed to induce and incorporate vascular networks within engineered bone constructs before implantation in order to achieve successful integration with the host tissue. Previous attempts to engineer vascularized bone tissue only focused on the effect of a single component among the three main components of TE (scaffold, cells, or signaling cues) and have only achieved limited success. However, with efforts to improve the engineered bone tissue substitutes, bone TE approaches have become more complex by combining multiple strategies simultaneously. The driving force behind combining various TE strategies is to produce bone replacements that more closely recapitulate human physiology. Here, we review and discuss the limitations of current bone TE approaches and possible strategies to improve vascularization in bone tissue substitutes.

## Introduction

**B**ONE TISSUE ENGINEERING (TE) has emerged with the aim of producing biological substitutes for bone tissue regeneration. The need for bone constructs stems from the limited availability of donor tissues, which can be categorized as autografts, allografts, and xenografts. However, each type of donor tissue comes with its own set of limitations. For example, many difficulties are associated with autografts, such as high cost, requirement of additional surgeries, donor-site morbidity, and limiting autografts for the treatment of small defects.<sup>1</sup> Allografts can be used for larger defects but are limited by the possible immune rejection, disease transmission, and lower incorporation rate

compared to autografts.<sup>1</sup> Xenografts are rarely used since they share the same drawbacks as allografts and their physiological structures and functions do not exactly match that of human tissue.<sup>2</sup> TE strategies have been applied as promising alternatives to address the problems associated with the current therapeutic techniques and to produce bone constructs that mimic the structure of natural bone.

In an attempt toward clinical success of engineered bone constructs, tissue engineers have focused on fabricating bone tissues with similar properties (e.g., mechanical strength and microstructure) and function to naturally occurring bone. Bone tissue is composed of an external layer, referred to as cortical or compact bone, and an internal layer, referred to as cancellous or spongy bone (Fig. 1). Cortical bone makes up to

<sup>1</sup>Harvard-MIT Division of Health Sciences and Technology, Massachusetts Institute of Technology, Cambridge, Massachusetts.

<sup>2</sup>Department of Medicine, Center for Biomedical Engineering, Brigham and Women's Hospital, Harvard Medical School, Cambridge, Massachusetts.

<sup>3</sup>École Polytechnique, Palaiseau, France.

<sup>4</sup>Department of Prosthodontics, Chonnam National University, Gwangju, South Korea.

<sup>5</sup>Department of Orthopedic Surgery, Stanford University, Stanford, California.

<sup>6</sup>World Premier International Advanced Institute for Materials Research (WPI-AIMR), Tohoku University, Sendai, Japan.

<sup>7</sup>Wyss Institute for Biologically Inspired Engineering, Harvard University, Boston, Massachusetts.

\*These two authors contributed equally to this work.

†Current affiliation: Department of Maxillofacial Biomedical Engineering and Institute of Oral Biology, School of Dentistry, Kyung Hee University, South Korea.

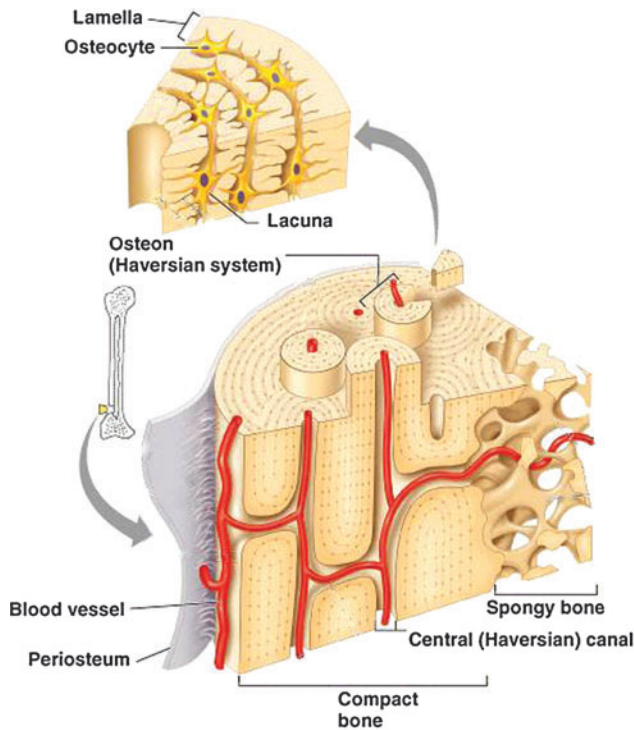


FIG. 1. Bone anatomy (Copyright © 2004 Pearson Education, Inc., publishing as Benjamin Cummings). Color images available online at [www.liebertpub.com/teb](http://www.liebertpub.com/teb)

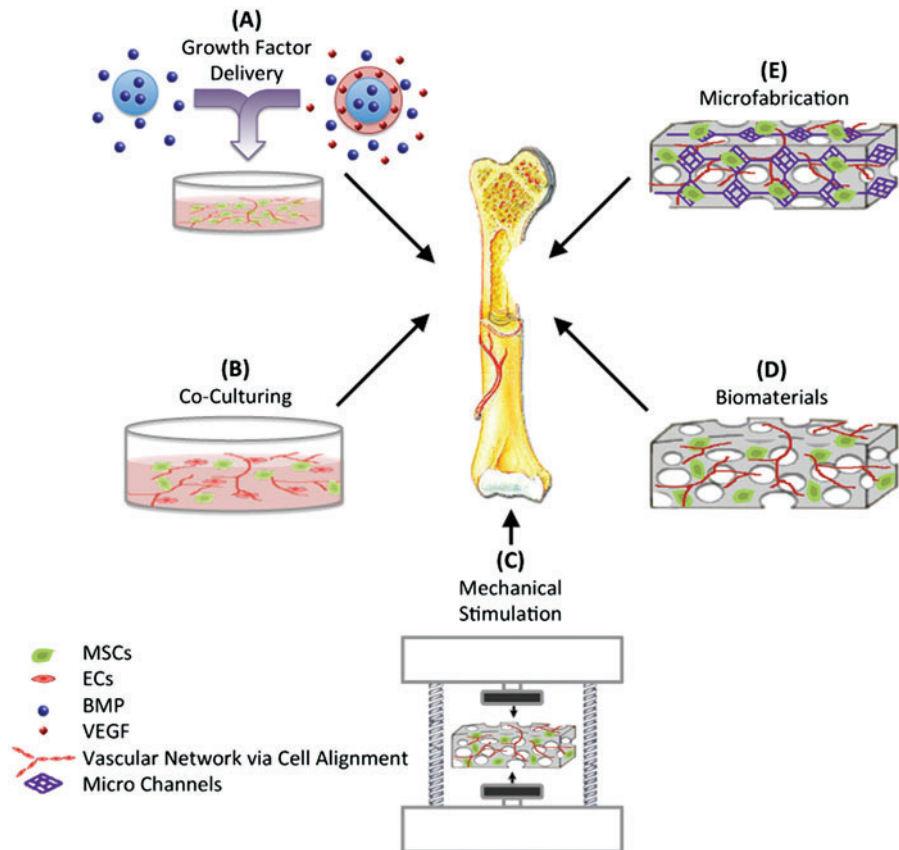
~80% of the total bone mass in adults.<sup>3</sup> It is extremely dense, with low porosity (20%) and high mechanical strength (130–190 MPa).<sup>4</sup> Cancellous bone accounts for the other 20% of the total bone mass and is highly porous (50%–90%), with ~10% of the mechanical strength of cortical bone.<sup>3</sup> Osteons are functional units within the cortical bone structure and contain central haversian canals, which house nerves and blood vessels.<sup>5</sup> In contrast, cancellous bone does not contain osteon units, as its high porosity and surface area allows for better penetration of vasculature.<sup>6</sup> Although cortical and cancellous layers are quite different in structure, they both contain a highly vascularized network. The presence of a vascular network is essential to supply nutrients and remove waste products. Therefore, it is required to incorporate a vascularized network into engineered bone substitutes in order to mimic the structure of natural bone tissue.

Despite their enormous potential for bone regeneration, current TE strategies are extremely limited by the lack of vascularization, leading to poor graft integration and failure of engineered substitutes in clinical trials. Here, we aim to discuss possible strategies to improve bone tissue regeneration by enhancement of vascularization in engineered constructs.

**Strategies to Enhance Vascularization in Engineered Bone Constructs**

Vascularization plays a crucial role in supplying cells with oxygen and nutrients and removing waste products from the engineered tissue constructs. The need for a vasculature is particularly important when engineering three-dimensional

FIG. 2. Various strategies to enhance vascularization in bone tissue engineering (TE). MSCs, mesenchymal stem cells; EC, endothelial cells; BMP, bone morphogenetic protein; VEGF, vascular endothelial growth factor. Color images available online at [www.liebertpub.com/teb](http://www.liebertpub.com/teb)



(3D) thick tissues like the heart, liver, and kidney.<sup>7-9</sup> The importance of vascularization has been also demonstrated for the engineering of other tissues, such as muscle, nerve, and bone.<sup>8,10,11</sup> Various strategies have been attempted to enhance the establishment of vascular networks within engineered constructs for bone regeneration (Fig. 2). These include (A) directing cell behavior through growth factor delivery, (B) using coculturing systems, (C) applying mechanical stimulation, (D) using biomaterials with appropriate properties, and (E) incorporating microfabrication techniques.

Interactions between cells play an important role in directing their function and differentiation. *In vivo* cellular communication is mainly through a cascade of chemical cues, such as protein interactions and growth factor signaling. Growth factors are known to affect cellular proliferation, migration, and differentiation during bone repair.<sup>12</sup> For instance, bone morphogenetic protein-2 (BMP-2), transforming growth factor- $\beta$  (TGF- $\beta$ ), fibroblast growth factor (FGF), platelet-derived growth factor (PDGF), insulin-like growth factor (IGF), endothelin-1, and vascular endothelial growth factor (VEGF) are involved in bone formation.<sup>13</sup> BMP, PDGF, FGF, and VEGF have been shown to enhance migration of osteoprogenitor cells, while TGF- $\beta$ , IGFs, and BMPs modulate their proliferation and differentiation.<sup>14</sup> Additionally, VEGF and FGF are involved in initiating vascular growth during bone healing.<sup>13</sup> The cross-talk between osteoblasts and endothelial cells (ECs) is conducted through the release of VEGF by osteoblasts, which act on ECs to promote angiogenesis,<sup>11</sup> and through the release of BMPs by ECs, which act on precursor bone cells to promote osteoblastic differentiation. In addition, FGF has been shown to stimulate proliferation and migration of ECs<sup>15</sup> and also induce osteoblast differentiation.<sup>16</sup> As for physical signals, cells can be stimulated either by cell-cell contact via coupling of gap junction proteins between different cell types or by externally applied stimulation such as mechanical or electrical signals. The coupling of osteocytes and ECs through gap junction proteins has been demonstrated to regulate gene expression and drive osteoblastic differentiation,<sup>17</sup> indicating the importance of cell-cell physical contact in directing cell function.

#### Growth factor delivery

As mentioned in the previous section, cells respond to chemical and physical signals; thus, previous bone TE approaches have exploited this concept to control cellular behavior both *in vitro* and *in vivo*. A number of investigators have attempted to recapitulate this signaling process *in vitro* through the delivery of exogenous growth factors to direct cellular behavior. The classic approach is to deliver one growth factor by bolus injection, but this approach does not emulate the *in vivo* cascade of cellular signaling. This is because bolus injections fail to locally and efficiently deliver specific growth factors for proper modulation of cellular function. Current efforts of bolus growth factor injection at the site of injury have been limited by the rapid diffusion of the growth factors and the lack of temporal control, resulting in nonlocalized and transient cellular responses. Tomanek *et al.* evaluated the effects of bolus injection of both VEGF and bFGF on vasculogenesis. It was found that the injection of VEGF induced inappropriate neovascularization in avascular areas.<sup>18</sup> The use of bFGF enhanced vasculogenesis, but the

vasculature was transient and disappeared at later stages.<sup>18</sup> As an alternative method to achieve sustained release of growth factors and in turn improve on bone TE strategies, investigators explored the effects of growth factor encapsulation within degradable microparticles. Solorio *et al.* encapsulated BMP-2 within crosslinked gelatin microparticles to induce bone formation from human mesenchymal stem cells (hMSCs) through the sustained release of BMP-2.<sup>19</sup> It was found that the release of BMP-2 from gelatin microparticles resulted in an increase of bone sialoprotein (BSP) gene expression of hMSCs.<sup>19</sup> In another study, Formiga *et al.* demonstrated that the sustained release of VEGF from poly (lactico-glycolic acid) (PLGA) microparticles resulted in *in vivo* revascularization with stable vessels.<sup>20</sup> However, vasculature was not formed through the bolus injection of free VEGF, which was due to the short half-life of the protein *in vivo*.

Furthermore, the delivery of a single growth factor often fails because its isolated action does not emulate the complex process of bone regeneration *in vivo*, which involves the interaction of a large number of growth factors and cytokines.<sup>21</sup> For this reason, a number of investigators have explored the effects of the combined delivery of multiple growth factors. BMPs are well established as potent osteoinductive growth factors and their delivery in combination with other growth factors has been shown to enhance bone formation *in vivo*.<sup>21</sup> A study by Duneas *et al.* demonstrated that the combination of TGF- $\beta$  and BMP-7 produced a synergistic effect to enhance bone formation *in vivo*.<sup>22</sup> This synergy was also observed by Simmons *et al.* after they implanted RGD-modified alginate hydrogels containing both TGF- $\beta$ 3 and BMP-2 with bone marrow stromal cells (BMSCs) in mice.<sup>23</sup> After 6 weeks of implantation, the combined delivery of both TGF- $\beta$ 3 and BMP-2 showed significant bone formation by transplanted BMSCs. In contrast, individual delivery of TGF- $\beta$ 3 or BMP-2 resulted in negligible bone formation even after 22 weeks. Interestingly, the enhancement of bone regeneration by the combined delivery of FGF and BMP is dependent on both time and dose. Kubota *et al.* combined the locally delivered BMP-2 with subcutaneous injections of FGF-4 and found that FGF increased bone formation when administered early (days 2-4), but had no effect when injected at later time points (days 6-11), demonstrating that the effect of FGF on BMP-induced bone formation is time dependent.<sup>24</sup> The dose-dependent effect of FGF when combined with BMP was observed by Nakamura *et al.* when they implanted type I collagen disks into mice that contained a constant amount of BMP-2 (5  $\mu$ g) and varying amounts of FGF-2.<sup>25</sup>

The effect of simultaneous and sequential delivery on bone formation has been also investigated.<sup>26-31</sup> In one study, Raiche *et al.* found that the temporal delivery of BMP-1 and IGF-I can significantly affect alkaline phosphatase (ALP) activity during *in vitro* culture.<sup>26</sup> In this study, layered gelatin coatings were used to develop a sequential delivery system; one layer was crosslinked to encapsulate BMP-2, while the other layer contained IGF-I. The highest ALP activity was observed with the early release of BMP-2 followed by the subsequent release of IGF-I, while the simultaneous release of BMP-2 and IGF-I from both layers had no effect on the ALP activity. Other studies have also shown the effect of sequential release of BMP-2 and BMP-7 from nanocapsules of PLGA and poly(3-hydroxybutyrate-co-3-hydroxyvalerate), and PLGA scaffolds loaded with poly(4-vinyl pyridine)/alginate acid polyelectrolyte microspheres.<sup>28,29</sup> It was found that

the early release of BMP-2 followed by BMP-7 suppressed rat MSC proliferation and increased osteogenic differentiation.<sup>28,29</sup> These results indicate that correct growth factor combinations and delivery strategies (simultaneous and sequential delivery, single or multiple growth factor) greatly affect osteogenic differentiation and should be considered when designing delivery systems.

The studies discussed above demonstrate that the delivery of multiple growth factors can enhance bone formation. However, since blood vessel formation is tightly coupled with bone regeneration, the ideal scenario would be to deliver a cascade of multiple growth factors to simultaneously induce angiogenesis and osteogenesis in order to produce a vascularized bone tissue substitute. VEGF plays a critical role in angiogenesis during bone formation; therefore, its combined delivery, along with other growth factors, may enhance vascularization in bone tissue constructs. In one study, Richardson *et al.* found that sustained dual delivery of both VEGF and PDGF resulted in highly dense and well-established vessels compared to the bolus delivery of either of the growth factors alone.<sup>32</sup> Patel *et al.* also demonstrated that dual delivery of VEGF and BMP-2 encapsulated in gelatin microparticles resulted in a synergistic effect, promoting both osteogenic response and blood vessel formation in an 8-mm rat cranial defect.<sup>33</sup> In another study, Shah *et al.* created a dual delivery system using polyelectrolyte multilayer films (PEM) fabricated through layer-by-layer assembly.<sup>34</sup> Various ratios of BMP-2 and VEGF were entrapped within the different PEM layers. It was found that VEGF was released from the PEM layers over the first 8 days, while the release of BMP-2 was sustained for 2 weeks. After implantation, the mineral density within *de novo* bone was increased by 33% in a PEM scaffold containing both BMP-2 and VEGF compared to those containing BMP-2 only. Mikos and coworkers also investigated the effects of individual and dual delivery of BMP-2 and VEGF on bone formation using a rat cranial critical-size defect.<sup>35</sup> Four weeks after implantation, dual delivery of BMP-2 and VEGF resulted in a higher percentage of bone fill compared to the delivery of BMP-2 alone. However, no significant difference was observed after 12 weeks.<sup>35</sup> These results suggest that the delivery of multiple growth factors is a possible strategy to enhance the formation of vascularized bone tissue substitutes. However, the types of growth factors to be combined, the dosage used, and the delivery method, all need to be carefully controlled in order to improve bone tissue formation, since slight alterations to any of these components can actually result in inhibition of bone regeneration. Furthermore, the limited number of studies on the combinatory delivery of multiple growth factors suggests the need of additional studies to evaluate all possible combinations and optimize concentrations, ratios, other timing, and delivery sequence.

### Coculturing systems

It is well known that there is an intricate connection between osteogenesis and angiogenesis during *in vivo* bone formation. In fact, angiogenesis is a prerequisite for osteogenesis.<sup>36</sup> Therefore, the cellular interaction between osteoblasts and ECs is essential in bone formation. Wang *et al.* illustrated the important relationship between osteoblasts and ECs by coculturing human osteoblast-like cells (HOBs) with human umbilical vein endothelial cells (HUVECs).<sup>37</sup> The co-

culture of HOBs with HUVECs resulted in an increase in both ALP activity and cell numbers. They also demonstrated that the release of VEGF by HOBs can be enhanced with 1,25-dihydroxyvitamin D3 induction, but this enhancement was only observed in cocultures of HOBs with HUVECs and not in HOBs cultured alone. The expression of VEGF receptors on ECs was also enhanced during coculture with HOBs, which resulted in stimulation of ALP activity. The release of VEGF by HOBs did not directly stimulate ALP activity, but in the presence of HUVECs, ALP stimulation was observed. The results of this study confirmed the importance of the communication between osteoblasts and ECs during osteogenesis.

As this review aims to discuss possible strategies for vascular enhancement within engineered bone tissue replacements, the coculture of ECs and osteoblasts is presented as a promising alternative, due to the important relationship between these cells during bone formation, remodeling, and repair.<sup>38</sup> Recent findings have shown that the *in vivo* vascular networks produced by a single-cell population are immature and less stable compared to networks formed from coculturing systems.<sup>39</sup> The importance of a coculturing system in bone TE stems from the need to promote osteogenesis and vascularization simultaneously in order to create vascularized engineered bone tissue constructs. Yu *et al.* demonstrated the feasibility of coculturing bone marrow-derived ECs and osteoblasts in a polycaprolactone (PCL)/hydroxyapatite scaffold to promote vascularization and osteogenesis processes.<sup>40</sup> It was found that the presence of both cell types within the scaffolds resulted in the formation of vessel-like structures.<sup>40</sup> In another study, Zhou *et al.* induced MSCs to differentiate into ECs, and then cocultured MSCs and MSC-derived ECs within a porous  $\beta$ -tricalcium phosphate ( $\beta$ -TCP) ceramic biomaterial to investigate the effects of MSC-derived ECs on the proliferation and osteogenesis of MSCs. Coculturing the cells resulted in vascularized bone formation, since ECs promoted MSCs osteogenesis and accelerated local vascularization. Additionally, *de novo* bone exhibited natural mechanical properties and vascularization after 16 weeks, with stable degradation of the implanted material and repair of bone defects within the rabbit model.<sup>41</sup> Villars *et al.* also demonstrated that coculturing of MSCs and ECs enhanced osteoblast proliferation and vascularization of engineered bone.<sup>17</sup> It was found that VEGF was not responsible for this improvement; the physical intercommunication involving cell membrane proteins between MSCs and ECs was the driving force of the superior cellular responses.<sup>17</sup> Kaigler *et al.* obtained similar results when they performed a comparative study that evaluated BMSCs cultured in ECs-conditioned medium, on ECs extracellular matrix (ECM), and cocultured with and without EC contact.<sup>42</sup> A significant increase in osteogenic differentiation of BMSCs was observed *in vitro* only when cultured in direct contact with ECs. Additionally, greater *in vivo* bone formation was detected when ECs were co-transplanted with BMSCs than when BMSCs were transplanted alone. These findings suggest that the use of coculturing systems can potentially aid in improving bone regeneration and enhancing preformed vascular networks for bone TE purposes.

### Mechanical stimulation

Mechanical force is a form of physical signaling that can affect cell functions within the body, including migration,

proliferation, enzyme secretion, and matrix orientation.<sup>43,44</sup> In bone TE, it has been well established that applying external mechanical stimuli can enhance bone tissue formation.<sup>45,46</sup> It has been shown that the use of bioreactors provides mechanical stimulation for cells to accelerate bone formation. They also induce fluid flow throughout the scaffold, allowing sufficient nutrient and waste exchange to increase cell viability and homogeneous distribution of cells within the biomaterial.<sup>47–49</sup> Various types of bioreactors such as spinner flask, rotating wall vessel reactor, and flow perfusion have been used to apply mechanical stimulation and fluid flow to bone tissue constructs and compare their effects with static culture conditions.<sup>48,49</sup> In one study, the effect of static and bioreactor cultures on PCL/TCP scaffolds seeded with human fetal MSC was investigated.<sup>48</sup> Compared to static culture, the use of a biaxial rotating bioreactor significantly increased proliferation and osteogenic differentiation both *in vitro* and *in vivo*, demonstrating its potential for bone TE applications.<sup>48</sup> In another study, a perfusion flow bioreactor was used to induce media perfusion and mechanical stimulations in a 3D culture condition for human bone mesenchymal stromal cells (hBMSC) encapsulated in a polyurethane scaffold.<sup>47</sup> *In vitro* studies indicated that the proliferation and differentiation of hBMSC were promoted when perfusion (10 mL/min) and on-off cyclic compressions mechanical stimulation (10% strain) were applied over 2 weeks' culture.<sup>47</sup> These results demonstrate that perfusion and mechanical stimulation, induced by using bioreactor, are promising approaches to enhance bone formation. Mauney *et al.* also demonstrated that the application of cyclic mechanical stimulation promoted osteogenic differentiation of MSCs within demineralized bone scaffolds.<sup>50</sup> Their developed bioreactor system closely mimicked the *in vivo* mechanical signals that stimulate osteoprogenitor cells to differentiate into osteoblasts within the cortical bone surface. Ignatius *et al.* also demonstrated that cyclic uniaxial mechanical strain increased multiple gene expressions that were involved in cell proliferation, matrix production, and osteoblastic differentiation.<sup>51</sup> Kaneuji *et al.* demonstrated that static compressive force enhanced the expression of osteoprotegerin, a known inhibitor of osteoclast differentiation, which resulted in the promotion of bone growth.<sup>46</sup> It was found that both osteoblasts and osteocytes respond to mechanical stress by regulating osteoclastogenesis.<sup>46</sup> In another study, Forwood *et al.* showed that dynamic load with a magnitude of 65 N increased bone formation rate and produced the highest osteogenic response.<sup>52</sup> However, they found that applying dynamic load did not affect the rate of bone formation until after 5 days of culture.<sup>52</sup> Van Eijk *et al.* verified the application of the load during the first 5 days of culture had a negative effect on cell proliferation and differentiation, while after day 5, the mechanical stimulation induced alignment, proliferation, and differentiation of bone marrow cells.<sup>53</sup> These findings suggested that the temporal regulation of the applied load plays a crucial role in regulating cell responses.

The use of mechanical stimulation to modulate MSC differentiation and osteocyte behavior has been well explored. However, to improve upon this strategy it may be crucial to understand how mechanical stimulation would affect ECs and their ability to form blood vessels *in vitro*. It has been shown that the initiation and progression of angiogenesis

processes, as well as ECs function, are affected by hemodynamic forces, which are exerted by blood flow (cyclic strain and shear stress).<sup>54,55</sup> For example, Von Offenbergs Sweeney *et al.* showed an increase in bovine aortic endothelial cell (BAEC) migration and tube formation as a function of applied strain,<sup>54</sup> while Li *et al.* found that BAEC proliferation was critically regulated by cyclic strain.<sup>55</sup> Additionally, Iba *et al.* demonstrated that cyclic strain influenced *in vitro* ECs alignment and elongation by a mechanism dependent on the organization and network of actin filaments.<sup>56</sup> Furthermore, Azuma *et al.* conducted a study to evaluate how BAECs respond to cyclic strain versus shear stress. They found a more robust and rapid activation of mechanoreceptors in response to shear stress than to cyclic strain, indicating that the type of mechanical force determines which mitogen-activated protein kinases are activated.<sup>57</sup> These studies provide evidence that mechanical stimuli not only affect osteogenesis but can also be utilized to initiate and regulate the process of angiogenesis and consequently lead to the formation of blood vessels.

Evidence from previous works shows that applying mechanical signals can help regulate one biological process, but like for any other *in vivo* phenomena, isolated responses do not occur. Few investigators have begun to study how mechanical stimulation would affect both osteogenesis and angiogenesis concurrently. Cheung *et al.* evaluated the relationship between fluid flow and osteocyte apoptosis and found that osteocytes, exposed to fluid flow, were protected from apoptosis.<sup>58</sup> Osteocyte apoptosis mainly occurred as a result of reduced interstitial fluid flow and preceded osteoclast recruitment and activity.<sup>59</sup> As a result, the colocalization of osteocyte apoptosis and the recruitment of osteoclasts at the remodeling site promoted angiogenesis, since the apoptosis of the osteocytes increased the release of VEGF. Cheung *et al.* also demonstrated that apoptotic osteocytes promoted EC proliferation, migration, and tubule network formation.<sup>58</sup> This study suggested that by regulating fluid flow, it is possible to modulate osteocyte apoptosis and promote vascularization in a VEGF-mediated manner. In another study, Li *et al.* developed a mechanical stimulator to apply periodic compressive load and evaluate VEGF delivery from alginate microparticles.<sup>60</sup> It was found that periodic compression accelerated VEGF release from alginate microspheres compared to noncompressed samples. Moreover, the applied load enhanced the expression of matrix metalloproteinase (MMP)-2 and -9 in HUVECs that were cultured on a demineralized bone scaffold containing VEGF alginate microspheres. The increased expression of MMPs suggested that enhanced release of VEGF under applied compressive load is crucial in HUVEC activation and angiogenesis promotion. The results of these studies illustrate the efforts toward combining TE strategies to further improve engineered constructs and to develop more complex tissue substitutes.

#### Utilization of suitable biomaterials

Another classical bone TE approach is to select a suitable biomaterial scaffold that provides structural support for 3D bone tissue formation.<sup>61</sup> The properties of scaffolds can be tailored in order to induce and direct cellular attachment, proliferation, migration, and differentiation,<sup>62</sup> making them prominent tools in the bone TE field. Table 1 summarizes

TABLE 1. EXAMPLES OF BIOMATERIALS USED FOR THE REGENERATION OF VASCULARIZED BONE TISSUE

Biomaterial	Pore size ( $\mu\text{m}$ )	Porosity (%)	Application	Refs.
PLG	250–425	—	VEGF delivery and regeneration of vascularized bone tissue	189
PLG	—	—	Sustained dual delivery of VEGF and PDGF resulted in highly dense and mature vessels	32
Starch/PCL	250	77	Human osteoblast-like cells <i>in vitro</i>	190
PLGA	25–400	95	MSC and VEC <i>in vitro</i> coculture, followed implantation in bilateral thigh defects in rat.	191
	—	—	Single hESC culture enhanced osteogenesis	192
	—	—	hESC and BMP achieved bone formation	193
	—	—	Sustained release of VEGF resulting in revascularization with stable vessels	20
Gelatin	—	—	Sustained release of BMP-2 increased BSP expression of hMSCs	19
	—	—	Dual delivery of VEGF and BMP-2 stimulated blood vessel formation and augmented osteogenic response	33
Alginate	—	—	Compressive load accelerated VEGF delivery and promoted MMP expression in HUVECs	60
Chitosan/polyester	—	—	Osteogenic differentiation of hMSCs	194
Hydroxyapatite	90–600	—	Ectopic bone formation in rat	131,195
	300–700	72–74	Vascular formation after implantation in Fascia lumbodorsalis defect in rabbit	136
PCL/hydroxyapatite	—	80	MSC and ECs <i>in vitro</i> coculture followed implantation in femur defects in mice.	196
	355–600	83	Coculture of ECs and osteoblasts promoted vascularization and osteogenesis and resulted in stable vessel-like structures	40
$\beta$ -TCP	—	—	Coculture of MSC-derived ECs and MSCs induced vascularized bone formation <i>in vivo</i>	41
PLGA/ $\beta$ -TCP	125–150	80–88	Rabbit calvarial defect	123
Polymeric foams containing hydroxyapatite	40–100	70–97	Rat osteoblast <i>in vitro</i>	130
Polyurethane	300–2000	85	Regeneration of bicortical defects in the iliac crest of estrogen-deficient sheep	77

PDGF, platelet-derived growth factor; BMP, bone morphogenetic protein; VEGF, vascular endothelial growth factor; ECs, endothelial cells; hMSC, human mesenchymal stem cells; BSP, bone sialoprotein; PLGA, poly (lactic-co-glycolic acid); HUVECs, human umbilical vein endothelial cells;  $\beta$ -TCP,  $\beta$ -tricalcium phosphate; PCL, polycaprolactone; MMP, matrix metalloproteinase; PLG, poly (L-lactide-co-glycolide); hESC, human embryonic stem cell.

examples of various biomaterials and their vascularization potential for bone tissue constructs.

Even though the use of biomaterial scaffolds in bone TE has shown success for bone regeneration, there are still some limitations. For example, lack of *de novo* tissue growth in 3D scaffolds remains a major limitation in clinical applications of engineered scaffolds for bone repair. The limited, peripheral bone tissue formation is mainly due to insufficient nutrient and oxygen delivery and metabolic waste removal within the 3D structure of the scaffolds.<sup>63,64</sup> This is more profound under static culture conditions, where the high cell density on the outer surfaces of the scaffolds may result in diminished nutrient supply to the cells located inside the scaffolds. Consequently, the cells at the center of the constructs would be subjected to nutrient deprivation and ultimately necrosis, which hinders the success of engineered constructs for bone regeneration.<sup>11,40</sup> In the absence of an intrinsic capillary network, the engineered tissues can only have a maximum thickness of 150–200  $\mu\text{m}$ ; dimensions larger than this threshold may result in lack of oxygen inside the biomaterials.<sup>65</sup>

In bone TE, biomaterial scaffolds serve as templates for bone-forming cell growth as well as the establishment of a

vascular system. Vasculature is formed through adhesion, migration, and functionality of ECs seeded within the scaffold. In fact, simultaneous *in vitro* culture of ECs and osteoblasts in a suitable scaffold can aid in the establishment of microcapillary-like networks within the constructs. The scaffold type and its properties play an important role in bone tissue formation as well as vascular network creation. The ability to fabricate scaffolds with the appropriate properties can help facilitate the formation of vasculature within the engineered bone constructs.

**Biomaterial selection.** Biomaterial selection is a critical factor in bone TE as the properties of scaffold mainly depend on the nature of the biomaterial. A variety of materials has been used in bone TE, including metals, ceramics, synthetic and natural polymers, and composites. The utilization of each individual material has been well explored by many investigators; however, the ability to identify the best biomaterial for bone TE applications is a difficult task, since each material has inherent drawbacks. Metals such as titanium, stainless steel, and cobalt-chromium can be used as biocompatible, strong, and inexpensive materials for bone repair. However, metals are not biodegradable and have

higher moduli than that of natural bone, which induces stress shielding.<sup>66,67</sup> Ceramics and biodegradable polymers have been investigated as alternative scaffolds for bone TE applications. Bioceramics such as hydroxyapatite and  $\beta$ -TCP have been widely used for bone repair due to their excellent bioactivity, which is attributed to their structural and compositional similarity with the mineral phase of bone.<sup>68</sup> The bioactivity of ceramics facilitates the attachment of osteoprogenitor cells seeded on the surface and production of bone ECM.<sup>69</sup> In spite of numerous advantages, the brittleness and low mechanical properties of ceramics may result in their fracture upon applying load, making them unsuitable for the regeneration of large bone defect.<sup>70-72</sup> In addition, the low degradation rate of bioceramics (e.g., hydroxyapatite) hinders the substitution of the scaffold with newly formed tissue after implantation. Although the fabrication of hydroxyapatite/ $\beta$ -TCP composite scaffolds (known as biphasic calcium phosphate [BCP]) increases the degradation rate, the BCP scaffolds still remain in the body for several months, which is longer than the required time for bone healing (a few weeks).<sup>69</sup>

Biodegradable polymers are ideal materials to use as alternatives to metals and ceramics for the development of bone TE scaffolds.<sup>73</sup> Their wide use for bone repair is due to their remarkable properties, including biocompatibility, tunable degradation, processability, and versatility.<sup>69</sup> Polymers are divided in two groups of natural and synthetic. Among synthetic polymers, poly ( $\alpha$ -hydroxy) esters, such as poly (lactic acid),<sup>74</sup> poly (glycolic acid),<sup>75</sup> PLGA,<sup>76</sup> and polyurethanes,<sup>77,78</sup> have been widely utilized for bone regeneration. Other synthetic polymers that are of interest for bone repair are poly (propylene fumarate) (PPF),<sup>79-82</sup> poly-anhydride,<sup>83,84</sup> and poly (ethylene oxide)/poly (butylene terephthalate) copolymers.<sup>85,86</sup> Synthetic biodegradable polymers have higher mechanical properties than natural polymers and can be easily processed. It is also possible to fabricate synthetic-based polymeric scaffolds with tunable properties, such mechanical stiffness and pore characteristics, to create an optimal environment for cell proliferation, vascularization, and new bone formation. However, the intrinsic hydrophobicity and lack of cell-recognition sites within the structures of some synthetic polymers obstruct cellular penetration, adhesion, and growth within the scaffold. Natural polymers can interact with cells to regulate or direct their function. However, they have lower mechanical properties compared to synthetic polymers. Common biopolymers used for bone regeneration include collagen,<sup>87</sup> silk fibroin,<sup>88</sup> chitosan,<sup>30,89</sup> starch,<sup>90,91</sup> hyaluronic acid,<sup>92</sup> and polyhydroxyalkanoates.<sup>93,94</sup>

Hydrogels are polymeric networks that have the ability to absorb and retain a large volume of water (80%–99%).<sup>95</sup> Hydrogels can be made from natural biodegradable polymers such collagen, chitosan, and gelatin, or synthetic polymers such as polyethylene glycol (PEG) and polyvinyl alcohol.<sup>96,97</sup> Their remarkable properties, including similarities with the ECM, proper biological performance, hydrophilicity, high permeability to oxygen and nutrients, and inherent cellular interaction capabilities, make them leading candidates for engineered tissue scaffolds.<sup>95</sup> However, they are mechanically weak and unable to support significant loads experienced by bone tissue *in vivo*. Various methods have been applied to enhance the mechanical properties of

hydrogels, such as crosslinking (chemical, physical, or UV)<sup>98,99</sup> or blending with other polymers.<sup>100-102</sup>

Limitations of individual materials have led investigators toward exploring ways to improve biomaterial characteristics, such as combining natural polymers with synthetic polymers to create a balance between biological signals and mechanical properties.<sup>103-106</sup> For instance, Annabi *et al.* developed a two-stage solvent-free dense gas technique to produce porous 3D structures of natural/synthetic polymeric composites.<sup>107</sup> In the first stage, a gas-foaming/salt-leaching process was used to create large pores with an average pore size of  $540 \pm 21 \mu\text{m}$  in a PCL matrix. The pores of PCL scaffolds were then filled with crosslinked elastin under high pressure  $\text{CO}_2$  to form an elastin structure (average pore size  $\sim 50 \mu\text{m}$ ) within the macroporous PCL scaffolds. The addition of elastin within the pores of PCL scaffolds improved the cellular attachment and proliferation within the constructs. The use of PCL also increased the compressive modulus, from 0.001 MPa for the pure elastin hydrogel, to 1.3 MPa.<sup>107</sup> A study conducted by Nguyen *et al.* demonstrated that the mechanical strength of natural polymers, such as chondroitin sulfate (82.4 kPa) and hyaluronic acid (31.5 kPa), could be improved to 118 and 331 kPa, respectively, by incorporating PEG, a synthetic polymer.<sup>104</sup> Additionally, polymers have been combined with ceramics to overcome the drawbacks of each individual material and provide composites that are suitable for osteogenic applications. For example, it was reported that the compressive modulus of a hydroxyapatite scaffold increased from 0.2 to 0.5 MPa when it was coated with PCL to create a hydroxyapatite/PCL composite.<sup>108</sup> Another study by Kang *et al.* also reported that infiltration of PLGA significantly increased the compressive strength of  $\beta$ -TCP scaffolds from 2.9 to 4.2 MPa, and toughness from 0.2 to 1.4 MPa, while retaining an interconnected and highly porous structure.<sup>109</sup> In addition, Lickorish *et al.* found that coating a collagen scaffold with hydroxyapatite could improve the attachment and proliferation of rabbit periosteal cells due to the formation of a bioactive apatite layer on the surface of the scaffold.<sup>110</sup> The combination of natural and synthetic polymers with ceramics has been also used in bone TE. Chen *et al.* developed a process to fabricate PLGA/collagen/apatite scaffolds with a porosity of 91% and pore sizes between 355 and 422  $\mu\text{m}$  for bone regeneration. In this technique, a porous structure of PLGA was first fabricated by using a salt-leaching process. Collagen microsponges were then formed in the pores of PLGA scaffold, followed by apatite particulate deposition on the surface of the microsponges. The use of PLGA improved the mechanical integrity of the scaffold and incorporation of collagen resulted in the uniform deposition of apatite particles throughout the scaffold, which enhanced bone formation.<sup>111</sup>

**Scaffold properties.** In bone TE, scaffolds serve as temporary structural supports for cell interactions and formation of bone ECM. Additionally, bone TE scaffolds have been used to deliver growth factors encapsulated within their structures,<sup>112</sup> and in some cases they have facilitated vascularization of neo-tissue.<sup>113,114</sup> In general, more successful biomaterial scaffolds for bone TE are biodegradable, biocompatible, porous, and possess sufficient mechanical strength for load-bearing applications. The scaffold characteristics, including porosity, average pore size, and

mechanical stiffness, have been shown to influence cell survival, signaling, growth, gene expression, and phenotype.<sup>115–118</sup> Many investigators have attempted to manipulate these properties to fabricate constructs, which mimic bone morphology, structure, and function.<sup>69</sup>

The pore architecture of scaffold in terms of porosity, average pore size, and pore interconnectivity is crucial for cell survival, proliferation, and formation of 3D bone tissue *in vitro* and *in vivo*.<sup>119</sup> The porosity of a scaffold can affect osteoblast proliferation and the extent of osteogenesis during bone regeneration<sup>120</sup>; thus, manipulating the porosity of the scaffold can improve scaffold function. Kuboki *et al.* reported that osteogenesis occurred when using a porous hydroxyapatite scaffold as a BMP-2 carrier in a rat ectopic model. However, no bone formation was observed when nonporous solid hydroxyapatite particles were used as the BMP-2 carriers.<sup>121</sup> In addition, scaffolds with highly porous surfaces enhance mechanical interconnection between the implanted biomaterial and surrounding bone tissue, resulting in higher mechanical stability at the implant/bone tissue interface.<sup>122</sup> Higher porosity and larger pore sizes have been also shown to allow for *in vivo* bone ingrowth and vascularization. Roy *et al.* found that in a PLGA/ $\beta$ -TCP composite scaffold with a porosity gradient from 80% to 88%, bone tissue formation was enhanced in the region with higher porosity after implantation in rabbit craniums.<sup>123</sup> Kruyt *et al.* also demonstrated higher proliferation of goat bone marrow stromal cells in hydroxyapatite scaffolds with 70% porosity and an average pore size of 800  $\mu\text{m}$  compared to those with 60% porosity and an average pore size of 700  $\mu\text{m}$  during a 6-day *ex vivo* culture.<sup>124</sup> However, *in vitro* osteogenesis has been shown to increase with lower porosity. Takahashi *et al.* fabricated nonwoven fabrics from polyethylene terephthalate (PET) with porosities ranging from 93% to 97%.<sup>125</sup> They reported that higher porosity (97%) allowed for sufficient oxygen and nutrient delivery within the scaffold, which resulted in an increase in the proliferation rate of rat MSCs. In contrast, MSCs cultured on PET scaffolds with lower porosity (93%) exhibited higher osteogenic differentiation.<sup>125</sup> These results demonstrated that scaffold porosity could be manipulated for better control and modulation of cellular behavior and function within the scaffold.

In addition to porosity, the average pore size of the scaffold greatly affects bone formation and the creation of a vascular network, and can also be manipulated to produce the desired outcomes. Pores are necessary for bone tissue formation as they allow for cell migration and ingrowth, and nutrient diffusion for cell survival. In general, scaffolds with pore sizes larger than 50  $\mu\text{m}$  can allow for both delivery of nutrients and oxygen and removal of metabolic waste, but can also result in lower cellular attachment and intracellular signaling, while scaffolds containing pore sizes smaller than 10  $\mu\text{m}$  have the opposite effects.<sup>126</sup> Therefore, the fabrication of scaffolds containing both macropores and micropores can be beneficial for bone formation and vasculature creation.<sup>127</sup> The initial study by Hulbert *et al.* demonstrated that optimum pore sizes should be larger than 100  $\mu\text{m}$  for regeneration of vascularized bone tissue.<sup>128</sup> In this study, calcium aluminate cylindrical pellets with 46% porosity and various pore sizes in the range of 10–200  $\mu\text{m}$  were implanted in dog femorals to investigate the effect of pore size on bone formation. They found that large pores (>200  $\mu\text{m}$ ) enhanced

bone ingrowth and vascular formation, while smaller pores, in the range of 75–100  $\mu\text{m}$ , resulted in formation of unmineralized osteoid tissue.<sup>128</sup> Further decrease in the pore sizes of the scaffolds (<75  $\mu\text{m}$ ) led to the formation of fibrous connective tissue after 12 weeks of implantation.<sup>128</sup> Narayan *et al.* also demonstrated that the average pore size and interpore distance of PLGA scaffold significantly influenced EC growth.<sup>129</sup> They reported that EC growth was enhanced on smaller pore sizes, in the range of 5–20  $\mu\text{m}$ , with lower interpore distance.<sup>129</sup> In another study, Akay *et al.* reported that the proliferation of primary rat osteoblasts seeded into a porous polymeric scaffold containing hydroxyapatite was enhanced when the average pore size of scaffold was less than 40  $\mu\text{m}$ .<sup>130</sup> Osteoblasts were shown to penetrate faster within the scaffolds containing large pores (>100  $\mu\text{m}$ ); however, the extent of mineralization was not affected by the pore size.<sup>130</sup> Kuboki *et al.* showed that higher bone formation occurred in porous hydroxyapatite scaffolds with pore sizes in the range of 300–400  $\mu\text{m}$  after 4 weeks of implantation in rat.<sup>131</sup> This was explained by the rapid vascularization within the implanted scaffolds, which provided a proper microenvironment for osteogenesis.<sup>131</sup> These results indicate that the average pore size of scaffolds can be manipulated to potentially improve the formation of bone and vascular networks in bone TE.

In addition to porosity and average pore size, pore interconnectivity within scaffolds also plays an important role in bone tissue formation. Lack of pore interconnection can lead to poor nutrient and oxygen delivery as well as limited waste removal from the scaffold.<sup>132</sup> This may inhibit cellular growth within the biomaterial even if it is highly porous. Gomes *et al.* studied the effect of pore interconnectivity and flow perfusion on the proliferation and osteogenic differentiation of rat BMSCs seeded on two starch-based scaffolds with different pores interconnectivities.<sup>133</sup> It was found that under perfusion flow, higher cell distribution was observed within the scaffolds with higher degree of pore interconnectivity compared to those with limited pore interconnects. Cells were not able to spread throughout the interior of the scaffold with low pore interconnectivity.<sup>133</sup> In another study, the effect of pore interconnections within silk fibroin scaffolds seeded with MSCs was investigated.<sup>134</sup> It was shown that the variation of pore interconnectivities had no significant effects on ALP expression and calcium deposition after 4 weeks of culture; however, cellular penetration and *in vitro* bone formation were significantly affected by scaffold interconnectivity. Silk scaffolds with highly interconnected pores allowed for homogenous mineralization and formation of bone-like tissue, while scaffolds with low degree of interconnectivity resulted in cellular growth only at the surface of the scaffolds.<sup>134</sup> Pamula *et al.* also showed that although gene expression levels of vinculin,  $\beta$ -actin, osteopontin, and osteocalcin were not affected by changing poly (L-lactide-co-glycolide) scaffold interconnectivities, faster colonization was observed in scaffolds with higher degree of interconnectivity.<sup>135</sup> Increasing the pore sizes and pore interconnectivities of scaffolds promoted proliferation of HOBs (MG-63) that were seeded on scaffolds up to 7 days of culture; however, these differences disappeared after 15 days of culture.<sup>135</sup>

The average pore size and pore interconnectivity of scaffolds have been also shown to affect vascularization within



bone tissue-engineered constructs.<sup>136,137</sup> Bai *et al.* used a combined template/casting technique to fabricate macroporous  $\beta$ -TCP scaffolds with controlled pore size and interconnections for vascularized bone tissue formation.<sup>136</sup> They showed that the pore architecture of the scaffold could affect vascularization when using a rabbit model. It was found that increasing the pore interconnectivity of the scaffold resulted in an increase in the size and number of the blood vessels formed within the macroporous scaffold, while an increase in scaffold pore size led to an augmentation in the size of blood vessels grown within the bioceramics. Scaffolds with pore sizes smaller than 400  $\mu\text{m}$  were shown to limit the growth of blood vessels within the biomaterial, while increasing the pore size above this value had no significant effect on vascular formation, suggesting an optimized pore size of 400  $\mu\text{m}$  for vascularization.<sup>136</sup> Ghanaati *et al.* also demonstrated that the pore size, porosity, and shape of  $\beta$ -TCP bone substitutes influenced the integration of the biomaterial within the defect site as well as vascularization rate, following implantation in Wistar rats.<sup>137</sup> The results of *in vivo* studies demonstrated that although high porosity (80%) allowed the penetration and growth of cells within the center of bone substitutes, the rate of vascularization was enhanced when the porosity of scaffold decreased from 80% to 40%. Ten days after implantation, the vascularization of scaffolds with low porosity was significantly higher than those with a high degree of porosity.<sup>137</sup> In another study, Klenke *et al.* studied the effect of pore size on the vascularization and osseointegration of ceramic scaffolds *in vivo*.<sup>138</sup> Porous ceramic scaffolds were fabricated by using a particle-leaching process with naphthalene particles followed by sintering. The fabricated ceramic scaffold had pores in the range of 40–280  $\mu\text{m}$ , depending on the sizes of naphthalene particles used during scaffold preparation. It was found that increasing the pore sizes of the scaffolds promoted vascular network formation within the material after implantation in mice. Vessel formation also occurred earlier in scaffolds with pore sizes larger than 140  $\mu\text{m}$ .<sup>138</sup> In addition, the functional capillary density, which indicated microvascular perfusion within the materials, increased when the pore sizes of the scaffold exceeded 140  $\mu\text{m}$ . The volume of newly formed bone tissues within the implant was also increased two-fold when the pore sizes increased from 40 to 280  $\mu\text{m}$ . These results demonstrate that the pore characteristics of the scaffolds play an important role in vascularization and osseointegration of bone substitutes.

**Gradient biomaterials.** Gradient biomaterials are scaffolds whose compositions and physical properties (e.g., stiffness, porosity, and topology) vary gradually and spatially.<sup>139</sup> A physical gradient is one characteristic that exists in several tissues, such as teeth, articular cartilage, and bone, as well as interfaces between different tissues, such as ligament-to-bone, cartilage-to-bone, and tendon-to-bone.<sup>139,140</sup> Bone tissue varies from a stiff and compact external structure (porosity 5%–30%), to a spongy internal configuration (porosity 30%–90%).<sup>141</sup> This gradient structure provides mechanical support to external loads while acting as a reservoir for bone marrow. Fabricating gradient scaffolds that mimic the microstructure of natural bone can potentially improve and enhance the formation of new bone tissue. In addition, the use of gradient scaffolds for bone TE can also potentially

increase the rate of vascularization and ingrowth of host vessels into the entire scaffold following implantation.

Generation of bone TE scaffolds with controlled spatial gradients provides a powerful tool for studying cell-biomaterial interactions in bone TE.<sup>142,143</sup> These gradient materials can improve cellular functions, including migration, signaling, proliferation, spreading, and differentiation. For example, the presence of a stiffness gradient has been shown to promote osteoblast development and function.<sup>127</sup> In one study, Marklein and Burdick fabricated a methacrylated hyaluronic acid scaffold with a 15-mm-long gradient in elastic modulus, ranging from 3 to 90 kPa. It was shown that hMSCs exhibited increased spreading and proliferation rates on the stiffer regions of scaffold compared to softer sections.<sup>144</sup> In another study, Oh *et al.* demonstrated that gradients in pore sizes and porosities could also influence cellular growth and bone tissue formation.<sup>126</sup> In this study, PCL scaffolds containing gradients in pore size ranging from 88 to 405  $\mu\text{m}$  and porosity in the range of 80%–94% were fabricated. *In vitro* studies demonstrated that the growth of osteoblast cells was promoted in the regions with pore sizes in the range of 380–405  $\mu\text{m}$ .<sup>126</sup> However, 4 weeks after implantation in rabbits, the scaffold region with 290–310  $\mu\text{m}$  pore size exhibited faster bone formation.<sup>126</sup>

To date, various methods have been applied to create gradient scaffolds for bone substitution.<sup>139</sup> Yang *et al.* developed a novel template-casting method to produce highly interconnected porous calcium phosphate (CaP)-graded scaffolds with controlled architecture, composition, and geometry.<sup>145–147</sup> In this technique, a paraffin template was first fabricated by filling two concentric polyethylene tubes with paraffin beads of two different sizes. The tubes containing paraffin beads were subsequently heated to 50°C to induce bead coalescence and formation of a unitary mold structure. The CaP slurry was cast into the preformed paraffin template, which was followed by solidifying, drying, and sintering processes to form the porous CaP scaffold. Using this technique, a graded CaP scaffold consisting of a dense external structure (~20% porosity) and a porous central structure (70% porosity) was fabricated (Fig. 3A, B).<sup>147</sup> It was demonstrated that the graded CaP scaffold had pore architectures and mechanical properties similar to natural bone. A porous CaP scaffold loaded with BMP-2 was implanted into a nude mouse to evaluate its ability to enhance bone formation and healing. It was found that the porous scaffolds loaded with BMP-2 induced ectopic bone formation after 1 month of implantation (Fig. 3C). The fabricated porous scaffolds were also used as BMP-2 carriers to induce bone formation in a 1.5-cm bone defect in rabbit. The results of radiography and micro-CT imaging exhibited the formation of new bone tissue after 1 month (Fig. 3D–F), demonstrating the ability of fabricated scaffolds to repair various bone defect models.<sup>146</sup>

In another study, PCL scaffolds with pore size and porosity gradients were formed by using a centrifuge method.<sup>126</sup> In this technique, a porous PCL scaffold was fabricated by centrifuging a cylindrical mold containing preformed fibril-like PCL, followed by heat-induced fibril bonding. The pore size and porosity of the fabricated scaffolds gradually increased along the longitudinal direction, due to the gradual increase of the centrifugal force along the cylindrical axis in the mold.<sup>126</sup> The pore size

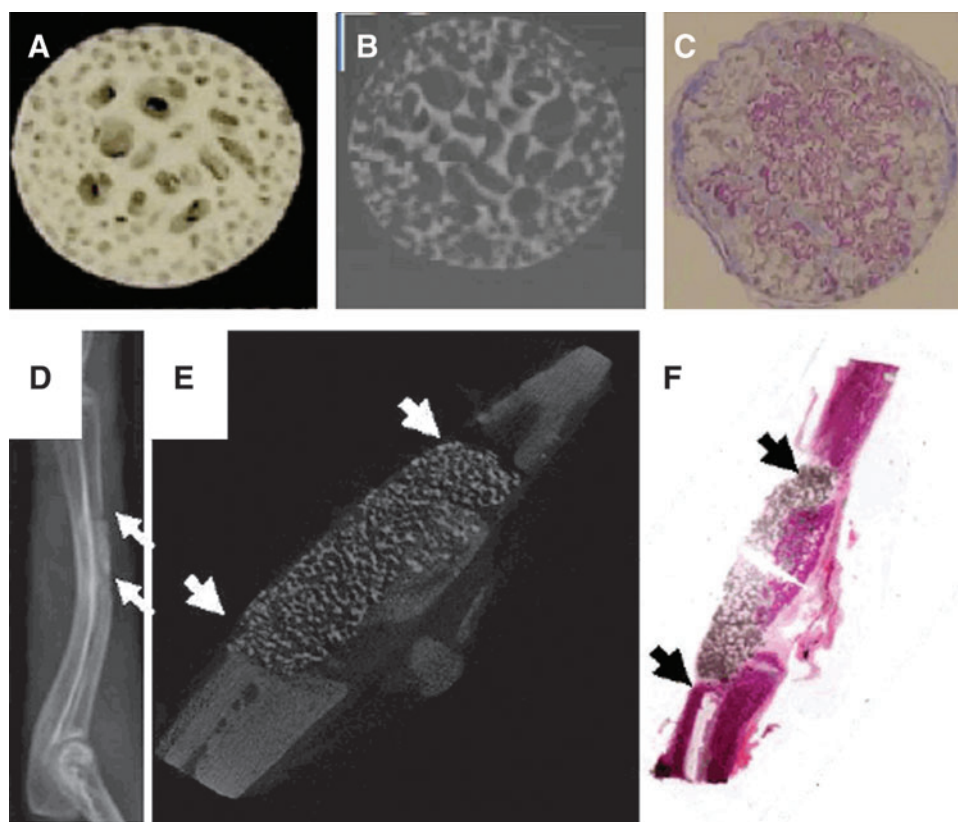


**FIG. 3.** Digital image (A) and two-dimensional micro-CT image (B) of calcium phosphate-graded scaffolds fabricated by using templating-casting method. The internal part of scaffold contained pores between 350 to 500  $\mu\text{m}$  in diameter and the external zone contained pores between 600 and 800  $\mu\text{m}$  (adapted with permission from Ref.<sup>187</sup>). (C) Histology images of bone morphogenetic protein (BMP)-2-induced ectopic bone formation in porous scaffold one month after implantation in nude mouse, demonstrating that the pores of scaffold were filled with newly formed bone, which is observed as the violet stain. (D) Radiography and (E) longitudinal micro-CT images of scaffold-aided bone healing at one month after implantation in a 1.5-cm bone defect in rabbit. (F) Longitudinal HE-stained histological image of a nondecalcified scaffold-bone sample. Arrows indicate the scaffold. Color images available online at [www.liebertpub.com/teb](http://www.liebertpub.com/teb)

gradient scaffolds were used to investigate the interaction between different cell types and scaffolds. It was found that various cell types required different pore size ranges for effective cellular growth. For example, chondrocytes and osteoblasts exhibited improved cell growth in the area of scaffold with larger pores, while fibroblast cells were shown to grow better in scaffold sections containing smaller pores.<sup>126</sup>

The fabrication of scaffold containing gradients of pore size, porosity, and stiffness that mimic the complex architecture of bone tissue provides a powerful tool for studying cell-biomaterial interactions to accelerate bone tissue regeneration. The fabrication of these complex gradient materials is another effort toward creating bone tissue constructs, and has potential to facilitate the formation of a bone-cartilage tissue interface. It is envisioned that the fabrication and design of gradient biomaterials will open a new avenue for regenerating vascularized bone tissues.

#### Microfabrication techniques

The previously discussed techniques (i.e., growth factors delivery, using a coculture system, and designing of novel biomaterials) have been widely used to improve the process

of vascularization for bone TE. However, these techniques usually result in the formation of randomly organized vessel networks with poor integration capability within the host organism. Therefore, it is desirable to utilize other techniques to preform host-like vessel networks within the cell-laden biomaterials. In the following sections, we discuss different techniques that allow development of more organized vessel networks that could potentially allow for the better integration with the host tissue.

**Microfabrication in bone TE.** Various techniques (e.g., electrospinning, twin screw extrusion, phase separation, and salt leaching) have been used to engineer biomimetic scaffolds for bone TE applications.<sup>143,148-153</sup> These techniques can be used to control the properties of scaffolds and have shown great potential for engineering bone tissue constructs. In addition, more advanced control on the cell microenvironment has been achieved through various microfabrication techniques. Using these technologies, it is possible to create microvasculature within engineered tissues to further improve integration with the host tissue.<sup>154</sup> Microscale technologies are the continuation of semiconductor and circuit technology, which comprise a wide range of processes to develop features in millimeter to submicrometer scales.<sup>155</sup>

The natural microenvironment of the cells *in vivo* is composed of numerous discrete chemical, mechanical, and topographical cues at the micro- and nanoscale, which are believed to serve as signaling mechanisms to control cell function.<sup>156,157</sup> Therefore, it may be possible to precisely control the cell microenvironment by integration of biology and microscale technologies in order to create engineered tissue constructs that comprise the complexity of the native tissue architectures.<sup>158</sup> To date, microscale technologies have been widely used to develop substrates, scaffolds, or biomaterials with specific properties to meet the desired criteria for bone TE applications. These technologies have also been employed in creating preformed vascular networks that can be ultimately incorporated within the biomaterials to deliver nutrition and oxygen and remove the waste products from the encapsulated cells.

Standard photolithography and soft lithography are among the common techniques that have been applied in patterning biomaterials to create cell-laden engineered tissue constructs. Standard photolithography usually requires a light-sensitive polymer solution containing a photoinitiator, a photomask layout, and a UV light source. The photomask is preprinted with the desired patterns and used to polymerize the polymer solution by exposing the patterned areas to UV light. The UV polymerization results in the cross-linking of the polymer solution to create a solid hydrogel with the desired patterns. Soft lithography techniques (i.e., microcontact printing and micromolding in capillaries) usually employ an elastomeric stamp, which is used to pattern the biomaterials with the desired geometrical features. Major advantages of soft lithography include simplicity and low cost, since these techniques do not require expensive clean room facilities. In addition, by using these techniques, it is possible to create patterns on a variety of planar or nonpla-

nar substrates.<sup>155,159</sup> Mata *et al.* used soft lithography to create microtextured surfaces on polydimethylsiloxane (PDMS) substrates to study the behavior of human bone marrow-derived cells (hBMDCs) under osteogenic culture conditions and evaluate their osteoblastic differentiation. The substrates were comprised of microchannels with curved surfaces separated by individual ridges (Fig. 4A). Differentiation of the hBMDCs toward the osteoblastic phenotype was confirmed through staining for ALP activity. On flat surfaces, hBMDCs were oriented in random directions forming large colonies, while on PDMS microchannels, the cells, which were mostly aligned, migrated along the channel axis and formed colonies with higher aspect ratios compared to those on flat surfaces. This technique can potentially be used to improve predesigned platforms and create implants with precise topographical features for bone TE applications.

Other studies have used microgrooves<sup>160–163</sup> and tapered micropits<sup>164</sup> as suitable topographies to address the current needs in bone TE. For example, Kirmizidis *et al.* used microgrooved features fabricated in polycarbonate to enhance alignment of primary calvarial rat osteoblast cells.<sup>163</sup> On grooves with 7  $\mu\text{m}$  depth and 10, 15, and 30  $\mu\text{m}$  widths, osteoblast cells exhibited a significantly improved alignment compared to flat surfaces. Notably, the cells maintained their cell–cell junctions (evaluated through connexin43 gap junction expression) and formed multilayers on 10- $\mu\text{m}$ -wide grooves, confirming that the proposed microscale topographies can be potentially used in designing suitable biomaterials for orthopedic implants.<sup>163</sup> In a similar work, a micromolding technique was employed to create hydroxyapatite-based grooved features to analyze human osteoblast cell alignment. The finding of this work indicated that narrow grooves (20  $\mu\text{m}$  width) significantly enhanced cellular orientation and alignment along their axis compared to wider grooves (40–100  $\mu\text{m}$

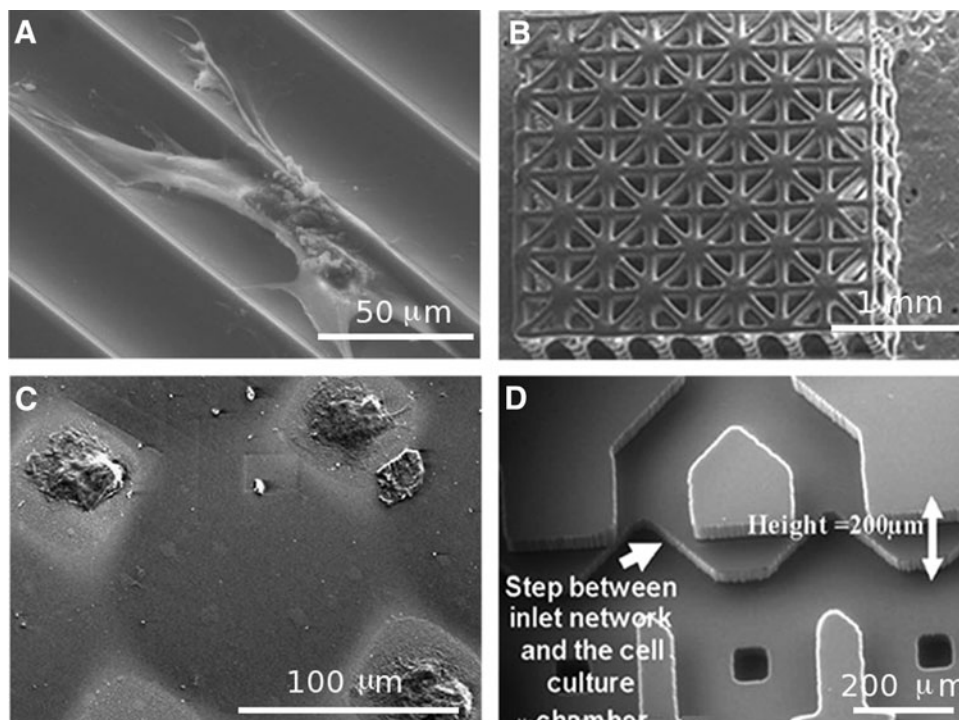


**FIG. 4.** SEM images of previously microfabricated platforms for bone TE applications. (A) Microfabricated PDMS channels; (B) three-dimensional scaffold fabricated with poly(propylene fumarate); (C) micropatterned polyethylene glycol (PEG) hydrogel on flat silicon surfaces; and (D) microfluidic network fabricated in polydimethylsiloxane (PDMS) (adapted with permission from Refs.<sup>166–168,188</sup>).

width).<sup>162</sup> Another study showed that on a tapered micropit topography, rat calvarial osteoblasts exhibited spindle line morphology and bridged the micropits, forming small adhesion sites, while mineralized tissue filled the area of the micropits upon *in vivo* implantation.<sup>163,164</sup>

Rapid prototyping techniques have been also used to develop 3D scaffolds for bone TE applications. Mapili *et al.* demonstrated a layer-by-layer microstereolithography technique to microfabricate complex and spatially patterned poly (ethylene glycol) dimethacrylate (PEGDMA) hydrogels with desired microfeatures for bone TE applications. Using this technique, it was possible to create 3D constructs with complex architectures and spatially distributed biomolecules (i.e., fibronectin-derived arginine-glycine-aspartic acid [RGD]). *In vitro* studies demonstrated enhanced attachment of murine bone marrow-derived stromal cells on the surfaces of the PEGDMA scaffolds.<sup>165</sup> A similar microstereolithography technique was also used to pattern PPF to create a 3D interconnected scaffold for bone TE applications (Fig. 4B).<sup>166</sup> The surface of the PPF scaffold was modified using biomimetic apatite and RGD to support cellular adhesion and migration. *In vitro* studies demonstrated that apatite-RGD-coated scaffolds provided a suitable microenvironment for the proliferation of preosteoblasts (MC3T3-E1) for up to 2 weeks. In another study, Subramani *et al.* used standard photolithography and microcontact printing to create anti-adhesive patterns of PEG hydrogel on planar silicon and glass surfaces with the desired geometrical features (Fig. 4C).<sup>167</sup> They seeded rat osteoblasts on the patterned substrates and found increased proliferation within the noncoated regions. Additionally, the incorporation of the VEGF within the PEG hydrogel induced osteoblast migration, indicating that osteoblast migration can be controlled using micropatterning techniques. The ability to control cellular migration and localize cellular proliferation with the use of growth factors and micropatterned substrates provides another potential solution for the development of vascularized bone implants.

Microfluidic devices have also been shown to be potentially advantageous in the field of bone TE. Leclerc *et al.* fabricated a 3D microfluidic device by assembling two PDMS layers, one containing microholes and microchambers to support cell adhesion and the other containing a fluid network (Fig. 4D).<sup>168</sup> Mouse calvarial osteoblastic cells (MC3T3-E1) were seeded within the device and subjected to static as well as dynamic culture conditions (flow rates of 5 and 35  $\mu\text{L}/\text{min}$ ). The cells were able to proliferate and attach within the microfluidic device under shear stress. Notably, MC3T3s cultured under the flow rate of 5  $\mu\text{L}/\text{min}$  exhibited a 7.5-fold increase in ALP activity compared to the cells in static culture condition.<sup>168</sup> The results of this study indicated that microfluidic devices can be used as efficient platforms for bone tissue regeneration. Although these PDMS-based devices cannot be utilized as implantable TE scaffolds, these systems can serve as proof-of-concept applications.

Applying microfabrication to potentially enhance vascularization in bone TE. The previous section focused on the use of microscale technologies to create scaffolds or substrates as suitable platforms for bone TE applications. This section will focus on the potential use of microfabrication techniques to enhance vascularization in engineered bone

substitutes. Microscale technologies hold a great promise in creating vascularized networks within engineered tissue constructs.<sup>9,169,170</sup> To date, numerous approaches such as micropatterning, microcontact printing, and micromolding have been widely adopted in the development of *in vitro* microscale vascularized networks.

A number of studies have used micropatterning of natural or synthetic hydrogels to enhance ECs alignment and promote angiogenesis.<sup>171–173</sup> West and coworkers have been actively involved in using microfabrication technologies and PEG-diacrylate (PEGDA) hydrogels to enhance the process of vascularization for TE applications. Standard photolithography techniques and laser scanning lithography were employed to pattern PEG hydrogels in the form of strips with variable width on a layer of PEGDA.<sup>173–176</sup> The surfaces of the patterned hydrogels have been modified through binding of cell-adhesive ligands (i.e., RGD), active molecules, and growth factors (i.e., VEGF) to support EC function. Their findings demonstrated that an intermediate concentration of RGD (20  $\mu\text{g}/\text{cm}^2$ ) induced HUVECs to undergo morphogenesis, assembling on top of each other to form cord-like structures along the patterned PEG strips.<sup>175</sup> Notably, the addition of VEGF to RGD ligands on the patterned hydrogel further enhanced tubule formation, which was verified by detecting lumens using confocal microscopy (Fig. 5A).<sup>173</sup> Khademhosseini and colleagues reported using methacrylated gelatin (GelMA) to investigate EC organization and alignment.<sup>171,177</sup> Gelatin is an inexpensive and biocompatible polymer that can be synthesized after hydrolysis of collagen, and maintains cell binding motifs, such as RGD, along its backbone. The methacrylation of gelatin makes it photocrosslinkable, and through microfabrication technology, it is possible to create patterned geometries on cell-laden GelMA hydrogels. In their work, they demonstrated that HUVECs were able to form lumen-like ring structures on GelMA with gel concentrations of 5%, 10%, and 15%.<sup>171</sup> Alignment of HUVECs was significantly enhanced within the patterned microchannels (50  $\mu\text{m}$  width) compared to unpatterned regions, confirming the possibility of creating 3D vascularized networks using micropatterned GelMA.<sup>177</sup>

Microcontact printing methods have been used to pattern proteins on two-dimensional surfaces in order to promote alignment and organization of ECs along the patterned regions.<sup>178,179</sup> The advantage of this technique is that patterns can be generated on a number of different substrates, such as glass, silicon, and polystyrene, using proteins solutions. This would allow for the creation of patterned microvasculature structures without consideration of the substrate materials.<sup>159</sup> For example, Dike *et al.* demonstrated that both human and bovine ECs were well-connected and differentiated, forming capillary-like structures comprised of luminal cavities when grown on 10- $\mu\text{m}$ -wide lanes.<sup>178</sup> In another approach, Gerecht and coworkers used microcontact printing followed by inversion of the patterned surfaces on a layer of fibrin hydrogel to promote tubulogenesis of human endothelial progenitor cells.<sup>179</sup> Fibronectin protein was patterned on glass substrates with widths in the range of 2.5 to 70  $\mu\text{m}$ . Optimal cell attachment and proliferation was observed on 50  $\mu\text{m}$  widths after 5 days of culture. The expression of adhesion molecules such as E-selectin and intercellular adhesion molecule-1 was significantly enhanced in response to tumor necrosis factor- $\alpha$ , indicating the angiogenic ability of

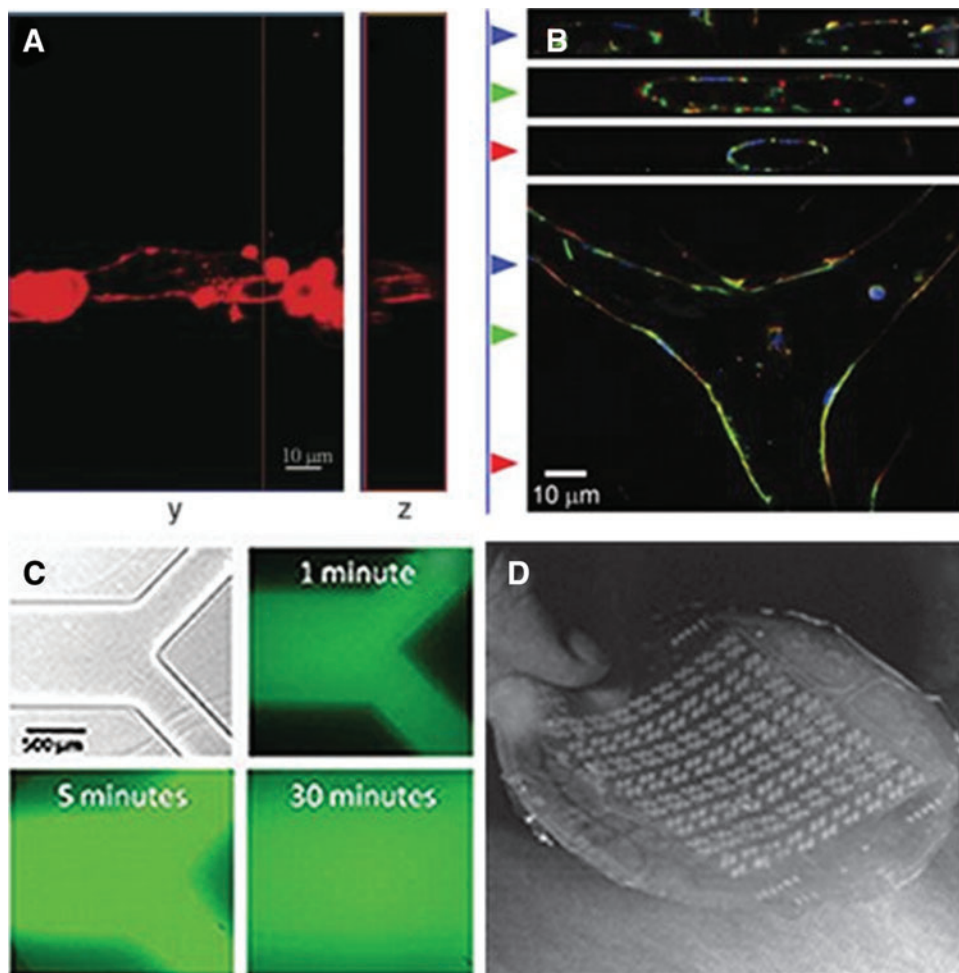


**FIG. 5.** (A) Top and cross-sectional confocal images of the actin filaments and tubule formation in endothelial cells (ECs) on PEG hydrogels patterned with RGDS and vascular endothelial growth factor. (B) Immunofluorescence images of ECs forming branched tubules using a micromolding technique. Actin filaments are stained in red, nuclei is stained in blue, and  $\beta$ -catenin is stained in green. (C) Microfluidic network fabricated in agarose hydrogels. (D) Highly branched microfluidic network fabricated in PDMS for vascularization applications (adapted with permission from Refs.<sup>173,180,181,185</sup>). Color images available online at [www.liebertpub.com/teb](http://www.liebertpub.com/teb)

the cells within the 50- $\mu$ m pattern widths. By addition of the fibrin gel to the patterned cells, it was possible to create 3D tubular structures comprising lumens.

Furthermore, other researchers have used micromolding techniques to spatially control EC organization and to enhance *in vitro* tubulogenesis. Raghavan *et al.* employed a micromolding technique to create cell-laden collagen gels consisting of microscale channels.<sup>180</sup> In this technique, a mold consisting of channels with the desired geometries and precoated with nonadhesive polymers was primarily fabricated in PDMS. The ECs were encapsulated within the collagen gel, and then the cell-laden gel was placed inside the channels through centrifugation followed by curing of collagen at 37°C. They observed that encapsulated ECs organized into tubes with lumens within 24–48 h.<sup>180</sup> It was also demonstrated that the tube diameter could be controlled by the collagen concentrations and channel width. Furthermore, the generation of more complex capillary architectures could be achieved by guiding the development of branches during tubule formation within the microfabricated geometry (Fig. 5B). These results illustrated the potential use of micromolding techniques to generate geometrically defined vascular networks.

In addition to micropatterning and micromolding of proteins and hydrogels, microfluidic systems have been used to develop 3D vascularized networks for TE applications. Both hydrogels<sup>181–183</sup> and biocompatible, biodegradable poly-

mers<sup>184,185</sup> have been used in development of microfluidic networks for vascularization purposes. In one study, soft lithography and a silicone master were used to mold the cell-embedded calcium alginate hydrogel on the desired microstructure.<sup>183</sup> Using this approach, it was possible to appropriately distribute the embedded microfluidic channels and uniformly exchange the soluble factors within bulk hydrogels. Khademhosseini and colleagues used a soft lithography technique to cast agarose hydrogels against a micropatterned SU-8 photoresist on a silicon substrate to create hydrogel-based microfluidic channels.<sup>181</sup> Subsequently, another layer of agarose hydrogel was used to seal the channels (Fig. 5C). They demonstrated that it was possible to create microfluidic channels with variable feature sizes and high porosity, which were suitable for the creation of vascular networks. Their results showed that the cells remained viable in close proximity of the channels, confirming proper nutrient and waste exchange through the channels to the surrounding regions.

Considerable work within this field has been done by Borenstein and colleagues to develop highly branched multilayer microfluidic network using biocompatible and biodegradable polymers such as PDMS<sup>185</sup> and PLGA<sup>184</sup> in order to mimic *in vivo* microvasculatures. In their primary studies, they used a patterned silicon substrate as a mold and replica-molding technique to create highly branched microfluidic network in PDMS, which was subsequently seeded

with ECs for vascular formation (Fig. 5D).<sup>185</sup> In another study, a PDMS mold was used to create the desired microstructures out of PLGA through a melt-molding process. Multiple layers of patterned PLGA layers were bonded through thermal fusion bonding to create the desired 3D multilayer microfluidic network.<sup>184</sup>

Microscale technologies have been proven to be a powerful tool in development of precise topographical features, scaffolds, and cell-laden hydrogels for bone TE applications. These technologies have been also applied to address the current challenges in vascularization of tissue constructs. Microscale technologies offer the flexibility in creating precise 3D architectures with embedded vascularized and capillary networks. For example, in a study by Moroni *et al.*, rapid prototyping computer-aided design/computer-aided manufacturing (CAD/CAM) was used to create microscale 3D scaffolds consisting of well-organized hollow fibers with controllable diameter and thickness that could be further used as a vascularized network for TE applications.<sup>186</sup> It is envisioned that by employing microscale technologies, it would be possible to address the current needs within the field of bone TE to produce a fully functional vascularized bone substitute.

## Conclusions

The direction of bone TE has evolved through the years, and as the progression developed, more advanced concepts are being incorporated into the equation. Novel approaches such as dual growth factor delivery, coculturing systems, incorporation of mechanical stimulation, biomaterials with tunable properties, and microfabrication of specific microfeatures, have been proposed in bone TE field to create constructs for generation of large bone defects. However, even with the development of these strategies, challenges still remain in the inability to reproduce an engineered bone replacement that truly mimics natural bone with well-formed and stable blood vessels. The lack of vascularization in engineered bone tissue is a major obstacle that needs to be overcome in order to achieve clinical success, particularly for the regeneration of large bone defects. The absence of a vascularized network limits the maximum effective size of engineered bone tissue due to insufficient nutrients and oxygen available within the constructs. The above-mentioned strategies have been proposed to enhance vascularization in bone tissue-engineered constructs. Although each individual approach does facilitate the formation of blood vessels, no one strategy alone has been successful in producing stable and mature vascularization within a bone replacement construct. Therefore, combining these approaches can be considered as a mean of further improvement toward generating vascularized bone tissue substitutes that more closely mimic the complexity of natural bone. The resulting engineered construct ideally would aid and facilitate the natural bone-healing process *in vivo*. The ability to accomplish such a complex native-like construct will bring the field of bone TE closer to the ultimate goal of producing a prevascularized bone tissue for the treatment of bone defects. With continued research in the techniques presented here, and new advanced techniques in the future, the improved ability to develop more complex bone tissue constructs will drive investigators closer to make advances toward clinical restoration of bone tissue function.

## Acknowledgments

This research has been supported by the NIH (HL092836, A.K.; EB008392, A.K.; DE019024, A.K.; HL099073, A.K.; AR057837, Y.Y.; DE021468, Y.Y.), NSF, A.K.; and DOD (W81XWH-10-1-0966, Y.Y.; W81XWH-10-200-10, Y.Y.; W81XWH-11-2-0168-P4, Y.Y.).

## Disclosure Statement

No competing financial interests exist.

## References

1. Salgado, A.J., Coutinho, O.P., and Reis, R.L. Bone tissue engineering: state of the art and future trends. *Macromol Biosci* **4**, 743, 2004.
2. Goldstein, S.A. Tissue engineering: functional assessment and clinical outcome. *Ann N Y Acad Sci* **961**, 183, 2002.
3. Sikavitsas, V.L., Temenoff, J.S., and Mikos, A.G. Biomaterials and bone mechanotransduction. *Biomaterials* **22**, 2581, 2001.
4. Turner, C.H., Wang, T., and Burr, D.B. Shear strength and fatigue properties of human cortical bone determined from pure shear tests. *Calcif Tissue Int* **69**, 373, 2001.
5. Hillier, M.L., and Bell, L.S. Differentiating human bone from animal bone: a review of histological methods. *J Forensic Sci* **52**, 249, 2007.
6. Rodan, G.A. Introduction to bone biology. *Bone* **13 Suppl 1**, S3, 1992.
7. He, W., Ye, L., Li, S., Liu, H., Wu, B., Wang, Q., Fu, X., Han, W., and Chen, Z. Construction of vascularized cardiac tissue from genetically modified mouse embryonic stem cells. *J Heart Lung Transplant* **31**, 204, 2012.
8. Jain, R.K., Au, P., Tam, J., Duda, D.G., and Fukumura, D. Engineering vascularized tissue. *Nat Biotechnol* **23**, 821, 2005.
9. Kaully, T., Kaufman-Francis, K., Lesman, A., and Levenberg, S. Vascularization: the conduit to viable engineered tissues. *Tissue Eng Part B Rev* **15**, 159, 2009.
10. Kermani, P., and Hempstead, B. Brain-derived neurotrophic factor: a newly described mediator of angiogenesis. *Trends Cardiovasc Med* **17**, 140, 2007.
11. Santos, M.I., and Reis, R.L. Vascularization in bone tissue engineering: physiology, current strategies, major hurdles and future challenges. *Macromol Biosci* **10**, 12, 2010.
12. Huang, Z., Nelson, E.R., Smith, R.L., and Goodman, S.B. The sequential expression profiles of growth factors from osteoprogenitors [correction of osteroprogenitors] to osteoblasts *in vitro*. *Tissue Eng* **13**, 2311, 2007.
13. Devescovi, V., Leonardi, E., Ciapetti, G., and Cenni, E. Growth factors in bone repair. *Chir Organi Mov* **92**, 161, 2008.
14. Malizos, K.N., and Papatheodorou, L.K. The healing potential of the periosteum molecular aspects. *Injury* **36 Suppl 3**, S13, 2005.
15. Collin-Osdoby, P., Rothe, L., Bekker, S., Anderson, F., Huang, Y., and Osdoby, P. Basic fibroblast growth factor stimulates osteoclast recruitment, development, and bone pit resorption in association with angiogenesis *in vivo* on the chick chorio-allantoic membrane and activates isolated avian osteoclast resorption *in vitro*. *J Bone Miner Res* **17**, 1859, 2002.
16. Kanczler, J.M., and Oreffo, R.O. Osteogenesis and angiogenesis: the potential for engineering bone. *Eur Cell Mater* **15**, 100, 2008.

17. Villars, F., Bordenave, L., Bareille, R., and Amedee, J. Effect of human endothelial cells on human bone marrow stromal cell phenotype: role of VEGF? *J Cell Biochem* **79**, 672, 2000.
18. Tomanek, R.J., Lotun, K., Clark, E.B., Suvarna, P.R., and Hu, N. VEGF and bFGF stimulate myocardial vascularization in embryonic chick. *Am J Physiol* **274**, H1620, 1998.
19. Solorio, L., Zwolinski, C., Lund, A.W., Farrell, M.J., and Stegemann, J.P. Gelatin microspheres crosslinked with genipin for local delivery of growth factors. *J Tissue Eng Regen Med* **4**, 514, 2010.
20. Formiga, F.R., Pelacho, B., Garbayo, E., Abizanda, G., Gavrira, J.J., Simon-Yarza, T., Mazo, M., Tamayo, E., Jauquicoa, C., Ortiz-de-Solorzano, C., Prosper, F., and Blanco-Prieto, M.J. Sustained release of VEGF through PLGA microparticles improves vasculogenesis and tissue remodeling in an acute myocardial ischemia-reperfusion model. *J Control Release* **147**, 30, 2010.
21. Kempen, D.H., Creemers, L.B., Alblas, J., Lu, L., Verbout, A.J., Yaszemski, M.J., and Dhert, W.J. Growth factor interactions in bone regeneration. *Tissue Eng Part B Rev* **16**, 551, 2010.
22. Duneas, N., Crooks, J., and Ripamonti, U. Transforming growth factor-beta 1: induction of bone morphogenetic protein genes expression during endochondral bone formation in the baboon, and synergistic interaction with osteogenic protein-1 (BMP-7). *Growth Factors* **15**, 259, 1998.
23. Simmons, C.A., Alsberg, E., Hsiong, S., Kim, W.J., and Mooney, D.J. Dual growth factor delivery and controlled scaffold degradation enhance *in vivo* bone formation by transplanted bone marrow stromal cells. *Bone* **35**, 562, 2004.
24. Kubota, K., Iseki, S., Kuroda, S., Oida, S., Imura, T., Duarte, W.R., Ohya, K., Ishikawa, I., and Kasugai, S. Synergistic effect of fibroblast growth factor-4 in ectopic bone formation induced by bone morphogenetic protein-2. *Bone* **31**, 465, 2002.
25. Nakamura, Y., Tensho, K., Nakaya, H., Nawata, M., Okabe, T., and Wakitani, S. Low dose fibroblast growth factor-2 (FGF-2) enhances bone morphogenetic protein-2 (BMP-2)-induced ectopic bone formation in mice. *Bone* **36**, 399, 2005.
26. Raiche, A.T., and Puleo, D.A. *In vitro* effects of combined and sequential delivery of two bone growth factors. *Biomaterials* **25**, 677, 2004.
27. Vo, T.N., Kasper, F.K., and Mikos, A.G. Strategies for controlled delivery of growth factors and cells for bone regeneration. *Adv Drug Deliv Rev* [Epub ahead of print]; DOI: 10.1016/j.addr.2012.01.016.
28. Buket Basmanav, F., Kose, G.T., and Hasirci, V. Sequential growth factor delivery from complexed microspheres for bone tissue engineering. *Biomaterials* **29**, 4195, 2008.
29. Yilgor, P., Hasirci, N., and Hasirci, V. Sequential BMP-2/BMP-7 delivery from polyester nanocapsules. *J Biomed Mater Res A* **93A**, 528, 2010.
30. Yilgor, P., Tuzlakoglu, K., Reis, R.L., Hasirci, N., and Hasirci, V. Incorporation of a sequential BMP-2/BMP-7 delivery system into chitosan-based scaffolds for bone tissue engineering. *Biomaterials* **30**, 3551, 2009.
31. Lee, K., Silva, E.A., and Mooney, D.J. Growth factor delivery-based tissue engineering: general approaches and a review of recent developments. *J R Soc Interface* **55**, 153, 2011.
32. Richardson, T.P., Peters, M.C., Ennett, A.B., and Mooney, D.J. Polymeric system for dual growth factor delivery. *Nat Biotech* **19**, 1029, 2001.
33. Patel, Z.S., Young, S., Tabata, Y., Jansen, J.A., Wong, M.E., and Mikos, A.G. Dual delivery of an angiogenic and an osteogenic growth factor for bone regeneration in a critical size defect model. *Bone* **43**, 931, 2008.
34. Shah, N.J., Macdonald, M.L., Beben, Y.M., Padera, R.F., Samuel, R.E., and Hammond, P.T. Tunable dual growth factor delivery from polyelectrolyte multilayer films. *Biomaterials* **32**, 6183, 2011.
35. Young, S., Patel Zarana, S., Kretlow James, D., Murphy Matthew, B., Mountziaris Paschalia, M., Baggett, L.S., Ueda, H., Tabata, Y., Jansen John, A., Wong, M., and Mikos Antonios, G. Dose effect of dual delivery of vascular endothelial growth factor and bone morphogenetic protein-2 on bone regeneration in a rat critical-size defect model. *Tissue Eng Part A* **15**, 2347, 2009.
36. McCarthy, I. The physiology of bone blood flow: a review. *J Bone Joint Surg Am* **88 Suppl 3**, 4, 2006.
37. Wang, D.S., Miura, M., Demura, H., and Sato, K. Anabolic effects of 1,25-dihydroxyvitamin D3 on osteoblasts are enhanced by vascular endothelial growth factor produced by osteoblasts and by growth factors produced by endothelial cells. *Endocrinol* **138**, 2953, 1997.
38. Samee, M., Kasugai, S., Kondo, H., Ohya, K., Shimokawa, H., and Kuroda, S. Bone morphogenetic protein-2 (BMP-2) and vascular endothelial growth factor (VEGF) transfection to human periosteal cells enhances osteoblast differentiation and bone formation. *J Pharmacol Sci* **108**, 18, 2008.
39. Koike, N., Fukumura, D., Gralla, O., Au, P., Schechner, J.S., and Jain, R.K. Tissue engineering: creation of long-lasting blood vessels. *Nature* **428**, 138, 2004.
40. Yu, H., VandeVord, P.J., Mao, L., Matthew, H.W., Wooley, P.H., and Yang, S.Y. Improved tissue-engineered bone regeneration by endothelial cell mediated vascularization. *Biomaterials* **30**, 508, 2009.
41. Zhou, J., Lin, H., Fang, T., Li, X., Dai, W., Uemura, T., and Dong, J. The repair of large segmental bone defects in the rabbit with vascularized tissue engineered bone. *Biomaterials* **31**, 1171, 2010.
42. Kaigler, D., Krebsbach, P.H., West, E.R., Horger, K., Huang, Y.C., and Mooney, D.J. Endothelial cell modulation of bone marrow stromal cell osteogenic potential. *FASEB J* **19**, 665, 2005.
43. Bell, E., Ivarsson, B., and Merrill, C. Production of a tissue-like structure by contraction of collagen lattices by human fibroblasts of different proliferative potential *in vitro*. *Proc Natl Acad Sci U S A* **76**, 1274, 1979.
44. Krishnan, L., Underwood, C.J., Maas, S., Ellis, B.J., Kode, T.C., Hoying, J.B., and Weiss, J.A. Effect of mechanical boundary conditions on orientation of angiogenic microvessels. *Cardiovasc Res* **78**, 324, 2008.
45. Huo, B., Lu, X.L., and Guo, X.E. Intercellular calcium wave propagation in linear and circuit-like bone cell networks. *Philos Transact A Math Phys Eng Sci* **368**, 617, 2010.
46. Kaneuji, T., Ariyoshi, W., Okinaga, T., Toshinaga, A., Takahashi, T., and Nishihara, T. Mechanisms involved in regulation of osteoclastic differentiation by mechanical stress-loaded osteoblasts. *Biochem Biophys Res Commun* **408**, 103, 2011.
47. Liu, C., Abedian, R., Meister, R., Haasper, C., Hurschler, C., Krettek, C., von Lewinski, G., and Jagodzinski, M. Influence of perfusion and compression on the proliferation and differentiation of bone mesenchymal stromal cells seeded on polyurethane scaffolds. *Biomaterials* **33**, 1052, 2012.

48. Zhang, Z.-Y., Teoh, S.H., Chong, W.-S., Foo, T.-T., Chng, Y.-C., Choolani, M., and Chan, J. A biaxial rotating bioreactor for the culture of fetal mesenchymal stem cells for bone tissue engineering. *Biomaterials* **30**, 2694, 2009.
49. Bancroft, G.N., Sikavitsas VI, and Mikos, A.G. Design of a flow perfusion bioreactor system for bone tissue-engineering applications. *Tissue Eng Part A* **9**, 549, 2003.
50. Mauney, J.R., Sjostrom, S., Blumberg, J., Horan, R., O'Leary, J.P., Vunjak-Novakovic, G., Volloch, V., and Kaplan, D.L. Mechanical stimulation promotes osteogenic differentiation of human bone marrow stromal cells on 3-D partially demineralized bone scaffolds *in vitro*. *Calcif Tissue Int* **74**, 458, 2004.
51. Ignatius, A., Blessing, H., Liedert, A., Schmidt, C., Neidlinger-Wilke, C., Kaspar, D., Friemert, B., and Claes, L. Tissue engineering of bone: effects of mechanical strain on osteoblastic cells in type I collagen matrices. *Biomaterials* **26**, 311, 2005.
52. Forwood, M.R., Owan, I., Takano, Y., and Turner, C.H. Increased bone formation in rat tibiae after a single short period of dynamic loading *in vivo*. *Am J Physiol* **270**, E419, 1996.
53. van Eijk, F., Saris, D.B., Creemers, L.B., Riesle, J., Willems, W.J., van Blitterswijk, C.A., Verbout, A.J., and Dhert, W.J. The effect of timing of mechanical stimulation on proliferation and differentiation of goat bone marrow stem cells cultured on braided PLGA scaffolds. *Tissue Eng Part A* **14**, 1425, 2008.
54. Von Offenberg Sweeney, N., Cummins, P.M., Cotter, E.J., Fitzpatrick, P.A., Birney, Y.A., Redmond, E.M., and Cahill, P.A. Cyclic strain-mediated regulation of vascular endothelial cell migration and tube formation. *Biochem Biophys Res Commun* **329**, 573, 2005.
55. Li, W., and Sumpio, B.E. Strain-induced vascular endothelial cell proliferation requires PI3K-dependent mTOR-4E-BP1 signal pathway. *Am J Physiol Heart Circ Physiol* **288**, H1591, 2005.
56. Iba, T., and Sumpio, B.E. Morphological response of human endothelial cells subjected to cyclic strain *in vitro*. *Microvasc Res* **42**, 245, 1991.
57. Azuma, N., Duzgun, S.A., Ikeda, M., Kito, H., Akasaka, N., Sasajima, T., and Sumpio, B.E. Endothelial cell response to different mechanical forces. *J Vasc Surg* **32**, 789, 2000.
58. Cheung, W.Y., Liu, C., Tonelli-Zasarsky, R.M., Simmons, C.A., and You, L. Osteocyte apoptosis is mechanically regulated and induces angiogenesis *in vitro*. *J Orthop Res* **29**, 523, 2011.
59. Aguirre, J.I., Plotkin, L.I., Stewart, S.A., Weinstein, R.S., Parfitt, A.M., Manolagas, S.C., and Bellido, T. Osteocyte apoptosis is induced by weightlessness in mice and precedes osteoclast recruitment and bone loss. *J Bone Miner Res* **21**, 605, 2006.
60. Li, Q., Hou, T., Zhao, J., and Xu, J. Vascular endothelial growth factor release from alginate microspheres under simulated physiological compressive loading and the effect on human vascular endothelial cells. *Tissue Eng Part A* **17**, 1777, 2011.
61. Rodrigues, M.T., Gomes, M.E., and Reis, R.L. Current strategies for osteochondral regeneration: from stem cells to pre-clinical approaches. *Curr Opin Biotechnol* **22**, 726, 2011.
62. Wojtowicz, A.M., Shekaran, A., Oest, M.E., Dupont, K.M., Templeman, K.L., Hutmacher, D.W., Guldberg, R.E., and Garcia, A.J. Coating of biomaterial scaffolds with the collagen-mimetic peptide GFOGER for bone defect repair. *Biomaterials* **31**, 2574, 2010.
63. Landman Kerry, A., and Cai Anna, Q. Cell proliferation and oxygen diffusion in a vascularising scaffold. *Bull Math Biol* **69**, 2405, 2007.
64. Sachlos, E., and Czernuszka, J.T. Making tissue engineering scaffolds work. *Euro Cells Mat* **5**, 29, 2003.
65. Fidkowski, C., Kaazempur-Mofrad, M.R., Borenstein, J., Vacanti, J.P., Langer, R., and Wang, Y. Endothelialized microvasculature based on a biodegradable elastomer. *Tissue Eng* **11**, 302, 2005.
66. Simon, J.A., Ricci, J.L., and Di Cesare, P.E. Bioresorbable fracture fixation in orthopedics: a comprehensive review. Part II. Clinical studies. *Am J Orthop (Belle Mead NJ)* **26**, 754, 1997.
67. Zhang, P., Hamamura, K., and Yokota, H. A brief review of bone adaptation to unloading. *J Proteomics Bioinform* **6**, 4, 2008.
68. El-Ghannam, A. Bone reconstruction: from bioceramics to tissue engineering. *Expert Rev Med Devices* **2**, 87, 2005.
69. Cordonnier, T., Sohier, J., Rosset, P., and Layrolle, P. Biomimetic materials for bone tissue engineering—state of the art and future trends. *Adv Biomater* **13**, B135, 2011.
70. Kohri, M., Miki, K., Waite, D.E., Nakajima, H., and Okabe, T. *In vitro* stability of biphasic calcium phosphate ceramics. *Biomaterials* **14**, 299, 1993.
71. Ducheyne, P. Bioceramics: material characteristics versus *in vivo* behavior. *J Biomed Mater Res* **21**, 219, 1987.
72. Rezwan, K., Chen, Q.Z., Blaker, J.J., and Boccaccini, A.R. Biodegradable and bioactive porous polymer/inorganic composite scaffolds for bone tissue engineering. *Biomaterials* **27**, 3413, 2006.
73. Agrawal, C.M., and Ray, R.B. Biodegradable polymeric scaffolds for musculoskeletal tissue engineering. *J Biomed Mater Res* **55**, 141, 2001.
74. Taboas, J.M., Maddox, R.D., Krebsbach, P.H., and Hollister, S.J. Indirect solid free form fabrication of local and global porous, biomimetic and composite 3D polymer-ceramic scaffolds. *Biomaterials* **24**, 181, 2002.
75. Agrawal, C.M., Best, J., Heckman, J.D., and Boyan, B.D. Protein release kinetics of a biodegradable implant for fracture non-unions. *J Biomed Mater* **16**, 1255, 1995.
76. Borden, M., El-Amin, S.F., Attawia, M., and Laurencin, C.T. Structural and human cellular assessment of a novel microsphere-based tissue engineered scaffold for bone repair. *J Biomed Mater* **24**, 597, 2002.
77. Gogolewski, S., Gorna, K., and Turner, A.S. Regeneration of bicortical defects in the iliac crest of estrogen-deficient sheep, using new biodegradable polyurethane bone graft substitutes. *J Biomed Mater Res A* **77A**, 802, 2006.
78. Laschke, M.W., Strohe, A., Scheuer, C., Eglin, D., Verrier, S., Alini, M., Pohlemann, T., and Menger, M.D. *In vivo* biocompatibility and vascularization of biodegradable porous polyurethane scaffolds for tissue engineering. *Acta Biomater* **5**, 1991, 2009.
79. Lewandrowski K.-U., Hile, D.D., Thompson, B.M.J., Wise, D.L., Tomford, W.W., and Trantolo, D.J. Quantitative measures of osteoinductivity of a porous poly(propylene fumarate) bone graft extender. *Tissue Eng* **9**, 85, 2003.
80. Vehof, J.W.M., Fisher, J.P., Dean, D., Van der Waerden J.-P.C.M., Spauwen, P.H.M., Mikos, A.G., and Jansen, J.A. Bone formation in transforming growth factor beta-1-coated porous poly(propylene fumarate) scaffolds. *J Biomed Mater Res* **60**, 241, 2002.



81. Fisher, J.P., Vehof, J.W.M., Dean, D., Van der Waerden J.P.C.M., Holland, T.A., Mikos, A.G., and Jansen, J.A. Soft and hard tissue response to photocrosslinked poly (propylene fumarate) scaffolds in a rabbit model. *J Biomed Mater Res* **59**, 547, 2002.
82. Fisher, J.P., Holland, T.A., Dean, D., Engel, P.S., and Mikos, A.G. Synthesis and properties of photocross-linked poly(propylene fumarate) scaffolds. *J Biomater Sci Polym Ed* **12**, 673, 2001.
83. Attawia, M.A., Uhrich, K., Herbert, K.M., Langer, R., and Laurencin, C.T. Long term osteoblast response to poly (anhydride-co-imides): a new degradable polymer for use in bone. *Proceedings of the Fifth World Biomaterials Congress, Toronto, Canada*, p. 113, 1996.
84. Ibim, S.E.M., Uhrich, K.E., Attawia, M., Shastri, V.R., El-Amin, S.F., Bronson, R., Langer, R., and Laurencin, C.T. Preliminary *in vivo* report on the osteocompatibility of poly(anhydride-co-imides) evaluated in a tibial model. *J Biomed Mater Res* **43**, 374, 1998.
85. Claese, M.B., Bruijn, J.D., Grijpma, D.W., and Feijen, J. Ectopic bone formation in cell-seeded poly(ethylene oxide)/poly(butylene terephthalate) copolymer scaffolds of varying porosity. *J Mater Sci Mater Med* **18**, 1299, 2007.
86. Kuijjer, R., Bouwmeester, S.J.M., Drees M.M.W.E., Surtel, D.A.M., Terwindt-Rouwenhorst, E.A.W., Van Der Linden, A.J., Van Blitterswijk, C.A., and Bulstra, S.K. The polymer polyactive as a bone-filling substance: an experimental study in rabbits. *J Mater Sci Mater Med* **9**, 449, 1998.
87. Rocha, L.B., Goissis, G., and Rossi, M.A. Biocompatibility of anionic collagen matrix as scaffold for bone healing. *Biomaterials* **23**, 449, 2001.
88. Nazarov, R., Jin, H.J., and Kaplan, D.L. Porous 3-D scaffolds from regenerated silk fibroin. *Biomacromolecules* **5**, 718, 2004.
89. Martins, A.M., Pham, Q.P., Malafaya, P.B., Raphael, R.M., Kasper, F.K., Reis, R.L., and Mikos, A.G. Natural stimulus responsive scaffolds/cells for bone tissue engineering: influence of lysozyme upon scaffold degradation and osteogenic differentiation of cultured marrow stromal cells induced by CaP coatings. *Tissue Eng Part A* **15**, 1953, 2009.
90. Gomes, M.E., Salgado, A., and Reis, R.L. Bone tissue engineering using starch based scaffolds obtained by different methods. *NATO Sci Ser II* **86**, 221, 2002.
91. Kunjachan, V., Subramanian, A., Hanna, M., and Guan, J.J. Comparison of different fabrication techniques used for processing 3-dimensional, porous, biodegradable scaffolds from modified starch for bone tissue engineering. *Biomed Sci Instrum* **40**, 129, 2004.
92. Kim, H.D., and Valentini, R.F. Retention and activity of BMP-2 in hyaluronic acid-based scaffolds *in vitro*. *J Biomed Mater Res* **59**, 573, 2002.
93. You, M., Peng, G., Li, J., Ma, P., Wang, Z., Shu, W., Peng, S., and Chen, G.-Q. Chondrogenic differentiation of human bone marrow mesenchymal stem cells on polyhydroxyalkanoate (PHA) scaffolds coated with PHA granule binding protein PhaP fused with RGD peptide. *Biomaterials* **32**, 2305, 2011.
94. Philip, S., Keshavarz, T., and Roy, I. Polyhydroxyalkanoates: biodegradable polymers with a range of applications. *J Chem Technol Biotechnol* **82**, 233, 2007.
95. Peppas, N.A., Hilt, J.Z., Khademhosseini, A., and Langer, R. Hydrogels in biology and medicine: from molecular principles to bionanotechnology. *Adv Mater* **18**, 1345, 2006.
96. Drury, J.L., and Mooney, D.J. Hydrogels for tissue engineering: scaffold design variables and applications. *Biomaterials* **24**, 4337, 2003.
97. Burdick, J.A., and Anseth, K.S. Photoencapsulation of osteoblasts in injectable RGD-modified PEG hydrogels for bone tissue engineering. *J Biomed Mater* **23**, 4315, 2002.
98. Lee, C.R., Grodzinsky, A.J., and Spector, M. The effects of cross-linking of collagen-glycosaminoglycan scaffolds on compressive stiffness, chondrocyte-mediated contraction, proliferation and biosynthesis. *Biomaterials* **22**, 3145, 2001.
99. Park, S.N., Park, J.C., Kim, H.O., Song, M.J., and Suh, H. Characterization of porous collagen/hyaluronic acid scaffold modified by 1-ethyl-3-(3-dimethylaminopropyl)carbodiimide cross-linking. *Biomaterials* **23**, 1205, 2002.
100. Tan, W., Krishnaraj, R., and Desai, T.A. Evaluation of nanostructured composite collagen—chitosan matrices for tissue engineering. *J Tissue Eng* **7**, 203, 2001.
101. Chen, G., Ushida, T., and Tateishi, T. Development of biodegradable porous scaffolds for tissue engineering. *Mater Sci Eng C Mater Biol Appl* **17**, 63, 2001.
102. Huang, L., Nagapudi, K., Apkarian, P.R., and Chaikof, E.L. Engineered collagen—PEO nanofibers and fabrics. *J Biomater Sci Polym Ed* **12**, 979, 2001.
103. Nguyen, L.H., Kudva, A.K., Saxena, N.S., and Roy, K. Engineering articular cartilage with spatially-varying matrix composition and mechanical properties from a single stem cell population using a multi-layered hydrogel. *Biomaterials* **32**, 6946, 2011.
104. Nguyen, L.H., Kudva, A.K., Guckert, N.L., Linse, K.D., and Roy, K. Unique biomaterial compositions direct bone marrow stem cells into specific chondrocytic phenotypes corresponding to the various zones of articular cartilage. *Biomaterials* **32**, 1327, 2011.
105. Rosa, A.L., de Oliveira, P.T., and Beloti, M.M. Macroporous scaffolds associated with cells to construct a hybrid biomaterial for bone tissue engineering. *Expert Rev Med Devices* **5**, 719, 2008.
106. Oliveira, A.L., and Reis, R.L. Pre-mineralization of starch/polycaprolactone bone tissue engineering scaffolds by a calcium-silicate-based process. *J Mater Sci Mater Med* **15**, 533, 2004.
107. Annabi, N., Fathi, A., Mithieux, S.M., Weiss, A.S., and Dehghani, F. Fabrication of porous PCL/elastin composite scaffolds for tissue engineering applications. *J Supercrit Fluids* **59**, 157, 2011.
108. Kim, H.-W., Knowles, J.C., and Kim, H.-E. Hydroxyapatite/poly(ε-CL) composite coatings on hydroxyapatite porous bone scaffold for drug delivery. *Biomaterials* **25**, 1279, 2003.
109. Kang, Y., Scully, A., Young, D.A., Kim, S., Tsao, H., Sen, M., and Yang, Y. Enhanced mechanical performance and biological evaluation of a PLGA coated beta-TCP composite scaffold for load-bearing applications. *Eur Polym J* **47**, 1569, 2011.
110. Lickorish, D., Ramshaw, J.A.M., Werkmeister, J.A., Glat-tauer, V., and Howlett, C.R. Collagen-hydroxyapatite composite prepared by biomimetic process. *J Biomed Mater Res A* **68**, 19, 2004.
111. Chen, G., Ushida, T., and Tateishi, T. Poly(DL-lactic-co-glycolic acid) sponge hybridized with collagen microsponges and deposited apatite particulates. *J Biomed Mater Res* **57**, 8, 2001.
112. Groeneveld, E.H.J., Van Den Bergh, J.P.A., Holzmann, P., Ten Bruggenkate, C.M., Tuinzing, D.B., and Burger, E.H.

- Mineralization processes in demineralized bone matrix grafts in human maxillary sinus floor elevations. *J Biomed Mater Res* **48**, 393, 1999.
113. Huttmacher, D.W. Scaffolds in tissue engineering bone and cartilage. *Biomaterials* **21**, 2529, 2000.
  114. Kneser, U., Voogd, A., Ohnolz, J., Buettner, O., Stangenberg, L., Zhang, Y.H., Stark, G.B., and Schaefer, D.J. Fibrin gel-immobilized primary osteoblasts in calcium phosphate bone cement: *in vivo* evaluation with regard to application as injectable biological bone substitute. *Cells Tissues Organs* **179**, 158, 2005.
  115. Leong, K.F., Cheah, C.M., and Chua, C.K. Solid freeform fabrication of three-dimensional scaffolds for engineering replacement tissues and organs. *Biomaterials* **24**, 2363, 2003.
  116. Desai, T.A. Micro- and nanoscale structures for tissue engineering constructs. *Med Eng Phys* **22**, 595, 2001.
  117. Webster, T.J., and Ejifor, J.U. Increased osteoblast adhesion on nanophase metals: Ti, Ti6Al4V, and CoCrMo. *Biomaterials* **25**, 4731, 2004.
  118. Popat, K.C., Daniels, R.H., Dubrow, R.S., Hardev, V., and Desai, T.A. Nanostructured surfaces for bone biotemplating applications. *Orthop Res Rev* **24**, 619, 2006.
  119. Mantila Roosa, S.M., Kempainen, J.M., Moffitt, E.N., Krebsbach, P.H., and Hollister, S.J. The pore size of polycaprolactone scaffolds has limited influence on bone regeneration in an *in vivo* model. *J Biomed Mater Res A* **92**, 359, 2010.
  120. Kasten, P., Beyen, I., Niemeyer, P., Luginbuhl, R., Bohner, M., and Richter, W. Porosity and pore size of beta-tricalcium phosphate scaffold can influence protein production and osteogenic differentiation of human mesenchymal stem cells: An *in vitro* and *in vivo* study. *Acta Biomater* **4**, 1904, 2008.
  121. Kuboki, Y., Takita, H., Kobayashi, D., Tsuruga, E., Inoue, M., Murata, M., Nagai, N., Dohi, Y., and Ohgushi, H. BMP-induced osteogenesis on the surface of hydroxyapatite with geometrically feasible and nonfeasible structures: Topology of osteogenesis. *J Biomed Mater Res* **39**, 190, 1998.
  122. Story, B.J., Wagner, W.R., Gaisser, D.M., Cook, S.D., and Rust-Dawicki, A.M. *In vivo* performance of a modified CSTi dental implant coating. *Int J Oral Maxillofac Implants* **13**, 749, 1998.
  123. Roy, T.D., Simon, J.L., Ricci, J.L., Rekow, E.D., Thompson, V.P., and Parsons, J.R. Performance of degradable composite bone repair products made via three-dimensional fabrication techniques. *J Biomed Mater Res* **66**, 283, 2003.
  124. Kruyt, M.C., De Bruijn, J.D., Wilson, C.E., Oner, F.C., Van Blitterswijk, C.A., Verbout, A.J., and Dhert, W.J.A. Viable osteogenic cells are obligatory for tissue-engineered ectopic bone formation in goats. *Tissue Eng* **9**, 327, 2003.
  125. Takahashi, Y., and Tabata, Y. Effect of the fiber diameter and porosity of non-woven PET fabrics on the osteogenic differentiation of mesenchymal stem cells. *J Biomater Sci Polym Ed* **15**, 41, 2004.
  126. Oh, S.H., Park, I.K., Kim, J.M., and Lee, J.H. *In vitro* and *in vivo* characteristics of PCL scaffolds with pore size gradient fabricated by a centrifugation method. *Biomaterials* **28**, 1664, 2007.
  127. Karageorgiou, V., and Kaplan, D. Porosity of 3D biomaterial scaffolds and osteogenesis. *Biomaterials* **26**, 5474, 2005.
  128. Hulbert, S.F., Young, F.A., Mathews, R.S., Klawitter, J.J., Talbert, C.D., and Stelling, F.H. Potential of ceramic materials as permanently implantable skeletal prostheses. *J Biomed Mater Res* **4**, 433, 1970.
  129. Narayan, D., and Venkatraman, S.S. Effect of pore size and interpore distance on endothelial cell growth on polymers. *J Biomed Mater Res A* **87A**, 710, 2008.
  130. Akay, G., Birch, M.A., and Bokhari, M.A. Microcellular polyHIPE polymer supports osteoblast growth and bone formation *in vitro*. *J Biomed Mater* **25**, 3991, 2004.
  131. Kuboki, Y., Jin, Q., and Takita, H. Geometry of carriers controlling phenotypic expression in BMP-induced osteogenesis and chondrogenesis. *Instr Course Lect* **83 A Suppl 1**, S105, 2001.
  132. Kim, K., Yeatts, A., Dean, D., and Fisher, J.P. Stereolithographic bone scaffold design parameters: osteogenic differentiation and signal expression. *Tissue Eng Part B* **16**, 523, 2010.
  133. Gomes, M.E., Sikavitsas, V.I., Behravesh, E., Reis, R.L., and Mikos, A.G. Effect of flow perfusion on the osteogenic differentiation of bone marrow stromal cells cultured on starch-based three-dimensional scaffolds. *J Biomed Mater Res* **67A**, 87, 2003.
  134. Uebersax, L., Hagenmuller, H., Hofmann, S., Gruenblatt, E., Muller, R., Vunjak-Novakovic, G., Kaplan, D.L., Merkle, H.P., and Meinel, L. Effect of scaffold design on bone morphology *in vitro*. *Tissue Eng* **12**, 3417, 2006.
  135. Pamula, E., Filova, E., Bacakova, L., Lisa, V., and Adamczyk, D. Resorbable polymeric scaffolds for bone tissue engineering: the influence of their microstructure on the growth of human osteoblast-like MG 63 cells. *J Biomed Mater Res A* **89A**, 432, 2009.
  136. Bai, F., Wang, Z., Lu, J., Liu, J., Chen, G., Lv, R., Wang, J., Lin, K., Zhang, J., and Huang, X. The correlation between the internal structure and vascularization of controllable porous bioceramic materials *in vivo*: a quantitative study. *Tissue Eng Part A* **16**, 3791, 2010.
  137. Ghanaati, S., Barbeck, M., Orth, C., Willershausen, I., Thimm, B.W., Hoffmann, C., Rasic, A., Sader, R.A., Unger, R.E., Peters, F., and Kirkpatrick, C.J. Influence of beta-tricalcium phosphate granule size and morphology on tissue reaction *in vivo*. *Acta Biomater* **6**, 4476, 2010.
  138. Klenke, F.M., Liu, Y., Yuan, H., Hunziker, E.B., Siebenrock, K.A., and Hofstetter, W. Impact of pore size on the vascularization and osseointegration of ceramic bone substitutes *in vivo*. *J Biomed Mater Res A* **85A**, 777, 2008.
  139. Sant, S., Hancock, M.J., Donnelly, J.P., Iyer, D., and Khademhosseini, A. Biomimetic gradient hydrogels for tissue engineering. *Can J Chem Eng* **88**, 899, 2010.
  140. Seidi, A., Ramalingam, M., Elloumi-Hannachi, I., Ostrovidov, S., and Khademhosseini, A. Gradient biomaterials for soft-to-hard interface tissue engineering. *Acta Biomater* **7**, 1441, 2011.
  141. Hall, S.J. *Basic Biomechanics*. Boston, MA: McGraw-Hill, 2007.
  142. Ozkan, S., Kalyon, D.M., and Yu, X. Functionally graded  $\beta$ -TCP/PCL nanocomposite scaffolds: *in vitro* evaluation with human fetal osteoblast cells for bone tissue engineering. *J Biomed Mater Res A* **92A**, 1007, 2010.
  143. Eriskin, C., Kalyon, D.M., and Wang, H. Functionally graded electrospun polycaprolactone and beta-tricalcium phosphate nanocomposites for tissue engineering applications. *Biomaterials* **29**, 4065, 2008.
  144. Marklein, R.A., and Burdick, J.A. Spatially controlled hydrogel mechanics to modulate stem cell interactions. *Soft Matter* **6**, 136, 2010.

145. Yang, Y., and Liu, Y. Method for making ceramic articles, including ceramic scaffolds for bone repair. US61/131, 810, 2008.
146. Yang, Y., and Liu, Y. Method for making ceramic articles, including ceramic scaffolds for bone repair. PCT/US 09/03501, 2009.
147. Liu, Y., Kim, J.-H., Young, D., Kim, S., Nishimoto, S.K., and Yang, Y. Novel template-casting technique for fabricating  $\beta$ -tricalcium phosphate scaffolds with high interconnectivity and mechanical strength and *in vitro* cell responses. *J Biomed Mater Res* **92A**, 997, 2010.
148. Shanti, R.M., Janjanin, S., Li, W.-J., Nesti, L.J., Mueller, M.B., Tzeng, M.B., and Tuan, R.S. In vitro adipose tissue engineering using an electrospun nanofibrous scaffold. *Ann Plast Surg* **61**, 566, 2008.
149. Jang, J.-H., Castano, O., and Kim, H.-W. Electrospun materials as potential platforms for bone tissue engineering. *Adv Drug Deliv Rev* **61**, 1065, 2009.
150. Zhang, X., Li, X., Fan, H., and Liu, X. Nano-hydroxyapatite/polymer composite scaffold for bone tissue engineering. *Key Eng Mater* **330**, 365, 2007.
151. Cevat, E., Dilhan, M.K., and Hongjun, W. A hybrid twin screw extrusion/electrospinning method to process nanoparticle-incorporated electrospun nanofibres. *Nanotechnol* **19**, 165302, 2008.
152. Ergun, A., Yu, X., Valdevit, A., Ritter, A., and Kalyon, D.M. *In vitro* analysis and mechanical properties of twin screw extruded single-layered and coextruded multilayered poly(caprolactone) scaffolds seeded with human fetal osteoblasts for bone tissue engineering. *J Biomed Mater Res A* **99A**, 354, 2011.
153. Ergun, A., Chung, R., Ward, D., Valdevit, A., Ritter, A., and Kalyon, D.M. Unitary bioresorbable cage/core bone graft substitutes for spinal arthrodesis coextruded from polycaprolactone biocomposites. *Ann Biomed Eng* **40**, 1073, 2011.
154. Andersson, H., and van den Berg, A. Microfabrication and microfluidics for tissue engineering: state of the art and future opportunities. *Lab Chip* **4**, 98, 2004.
155. Whitesides, G.M., Ostuni, E., Takayama, S., Jiang, X., and Ingber, D.E. Soft lithography in biology and biochemistry. *Annu Rev Biomed Eng* **3**, 335, 2001.
156. Goodman, S.L., Sims, P.A., and Albrecht, R.M. Three-dimensional extracellular matrix textured biomaterials. *Biomaterials* **17**, 2087, 1996.
157. Abrams, G.A., Goodman, S.L., Nealey, P.F., Franco, M., and Murphy, C.J. Nanoscale topography of the basement membrane underlying the corneal epithelium of the rhesus macaque. *Cell Tissue Res* **299**, 39, 2000.
158. Park, T.H., and Shuler, M.L. Integration of cell culture and microfabrication technology. *Biotechnol Prog* **19**, 243, 2003.
159. Kane, R.S., Takayama, S., Ostuni, E., Ingber, D.E., and Whitesides, G.M. Patterning proteins and cells using soft lithography. *Biomaterials* **20**, 2363, 1999.
160. Lu, X., and Leng, Y. Comparison of the osteoblast and myoblast behavior on hydroxyapatite microgrooves. *J Biomed Mater Res B Appl Biomater* **90B**, 438, 2009.
161. Lu, X., and Leng, Y. Quantitative analysis of osteoblast behavior on microgrooved hydroxyapatite and titanium substrata. *J Biomed Mater Res* **66A**, 677, 2003.
162. Holthaus, M.G., Stolle, J., Treccani, L., and Rezwani, K. Orientation of human osteoblasts on hydroxyapatite-based microchannels. *Acta Biomater* **8**, 394, 2012.
163. Kirmizidis, G., and Birch, M. Microfabricated grooved substrates influence cell-cell communication and osteoblast differentiation *in vitro*. *Tissue Eng Part A* **15**, 1427, 2009.
164. Hamilton, D.W., Chehroudi, B., and Brunette, D.M. Comparative response of epithelial cells and osteoblasts to microfabricated tapered pit topographies *in vitro* and *in vivo*. *Biomaterials* **28**, 2281, 2007.
165. Mapili, G., Lu, Y., Chen, S., and Roy, K. Laser-layered microfabrication of spatially patterned functionalized tissue-engineering scaffolds. *J Biomed Mater Res B Appl Biomater* **75**, 414, 2005.
166. Lan, P.X., Lee, J.W., Seol, Y.J., and Cho, D.W. Development of 3D PPF/DEF scaffolds using micro-stereolithography and surface modification. *J Mater Sci Mater Med* **20**, 271, 2009.
167. Subramani, K., and Birch, M.A. Fabrication of poly(ethylene glycol) hydrogel micropatterns with osteoinductive growth factors and evaluation of the effects on osteoblast activity and function. *Biomed Mater* **1**, 144, 2006.
168. Leclerc, E., David, B., Griscom, L., Lepioufle, B., Fujii, T., Layrolle, P., and Legallais, C. Study of osteoblastic cells in a microfluidic environment. *Biomaterials* **27**, 586, 2006.
169. Lovett, M., Lee, K., Edwards, A., and Kaplan, D.L. Vascularization strategies for tissue engineering. *Tissue Eng Part B* **15**, 353, 2009.
170. Moon, J.J., and West, J.L. Vascularization of engineered tissues: approaches to promote angiogenesis in biomaterials. *Curr Top Med Chem* **8**, 300, 2008.
171. Nichol, J.W., Koshy, S.T., Bae, H., Hwang, C.M., Yamanlar, S., and Khademhosseini, A. Cell-laden micro-engineered gelatin methacrylate hydrogels. *Biomaterials* **31**, 5536, 2010.
172. Hahn, M.S., Miller, J.S., and West, J.L. Three-dimensional biochemical and biomechanical patterning of hydrogels for guiding cell behavior. *Adv Mater* **18**, 2679, 2006.
173. Leslie-Barbick, J.E., Shen, C., Chen, C., and West, J.L. Micron-scale spatially patterned, covalently immobilized vascular endothelial growth factor on hydrogels accelerates endothelial tubulogenesis and increases cellular angiogenic responses. *Tissue Eng Part A* **17**, 221, 2011.
174. Hahn, M.S., Taite, L.J., Moon, J.J., Rowland, M.C., Ruffino, K.A., and West, J.L. Photolithographic patterning of polyethylene glycol hydrogels. *Biomaterials* **27**, 2519, 2006.
175. Moon, J.J., Hahn, M.S., Kim, I., Nsiah, B.A., and West, J.L. Micropatterning of poly(ethylene glycol) diacrylate hydrogels with biomolecules to regulate and guide endothelial morphogenesis. *Tissue Eng Part A* **15**, 579, 2009.
176. Moon, J.J., Saik, J.E., Poche, R.A., Leslie-Barbick, J.E., Lee, S.H., Smith, A.A., Dickinson, M.E., and West, J.L. Biomimetic hydrogels with pro-angiogenic properties. *Biomaterials* **31**, 3840, 2010.
177. Aubin, H., Nichol, J.W., Hutson, C.B., Bae, H., Sieminski, A.L., Crokek, D.M., Akhyari, P., and Khademhosseini, A. Directed 3D cell alignment and elongation in micro-engineered hydrogels. *Biomaterials* **31**, 6941, 2010.
178. Dike, L.E., Chen, C.S., Mrksich, M., Tien, J., Whitesides, G.M., and Ingber, D.E. Geometric control of switching between growth, apoptosis, and differentiation during angiogenesis using micropatterned substrates. *In Vitro Cell Dev Biol Anim* **35**, 441, 1999.
179. Dickinson, L.E., Moura, M.E., and Gerecht, S. Guiding endothelial progenitor cell tube formation using patterned fibronectin surfaces. *Soft Matter* **6**, 5109, 2010.
180. Raghavan, S., Nelson, C.M., Baranski, J.D., Lim, E., and Chen, C.S. Geometrically controlled endothelial tubulogenesis in micropatterned gels. *Tissue Eng Part A* **16**, 2255, 2010.

181. Ling, Y., Rubin, J., Deng, Y., Huang, C., Demirci, U., Karp, J.M., and Khademhosseini, A. A cell-laden microfluidic hydrogel. *Lab Chip* **7**, 756, 2007.
182. Golden, A.P., and Tien, J. Fabrication of microfluidic hydrogels using molded gelatin as a sacrificial element. *Lab Chip* **7**, 720, 2007.
183. Choi, N.W., Cabodi, M., Held, B., Gleghorn, J.P., Bonassar, L.J., and Stroock, A.D. Microfluidic scaffolds for tissue engineering. *Nat Mater* **6**, 908, 2007.
184. King, K.R., Wang, C.C.J., Kaazempur-Mofrad, M.R., Vacanti, J.P., and Borenstein, J.T. Biodegradable microfluidics. *Adv Mater* **16**, 2007, 2004.
185. Borenstein, J.T., Terai, H., King, K.R., Weinberg, E.J., Kaazempur-Mofrad, M.R., and Vacanti, J.P. Microfabrication technology for vascularized tissue engineering. *Biomed Microdevices* **4**, 167, 2002.
186. Moroni, L., Schotel, R., Sohler, J., de Wijn, J.R., and van Blitterswijk, C.A. Polymer hollow fiber three-dimensional matrices with controllable cavity and shell thickness. *Biomaterials* **27**, 5918, 2006.
187. Yang, Y., Kang, Y., Sen, M., and Park, S. Bioceramics in tissue engineering. In: Burdick, J.A., and Mauck, R.L., ed. *Biomaterials for Tissue Engineering: A Review of the Past and Future Trends*. New York: Springer Wien New York, 2010, pp. 179.
188. Mata, A., Boehm, C., Fleischman, A.J., Muschler, G., and Roy, S. Analysis of connective tissue progenitor cell behavior on polydimethylsiloxane smooth and channel micro-textures. *Biomed Microdevices* **4**, 267, 2002.
189. Murphy, W.L., Peters, M.C., Kohn, D.H., and Mooney, D.J. Sustained release of vascular endothelial growth factor from mineralized poly(lactide-co-glycolide) scaffolds for tissue engineering. *Biomaterials* **21**, 2521, 2000.
190. Tuzlakoglu, K., Pashkuleva, I., Rodrigues, M.T., Gomes, M.E., van Lenthe, G.H., Müller, R., and Reis, R.L. A new route to produce starch-based fiber mesh scaffolds by wet spinning and subsequent surface modification as a way to improve cell attachment and proliferation. *J Biomed Mater Res A* **92A**, 369, 2010.
191. Sun, H., Qu, Z., Guo, Y., Zang, G., and Yang, B. *In vitro* and *in vivo* effects of rat kidney vascular endothelial cells on osteogenesis of rat bone marrow mesenchymal stem cells growing on polylactide-glycolic acid (PLGA) scaffolds. *Biomed Eng Online* **6**, 41, 2007.
192. Tian, X.F., Heng, B.C., Ge, Z., Lu, K., Rufaihah, A.J., Fan, V.T., Yeo, J.F., and Cao, T. Comparison of osteogenesis of human embryonic stem cells within 2D and 3D culture systems. *Scand J Clin Lab Invest* **68**, 58, 2008.
193. Kim, S., Kim, S.S., Lee, S.H., Eun Ahn, S., Gwak, S.J., Song, J.H., Kim, B.S., and Chung, H.M. *In vivo* bone formation from human embryonic stem cell-derived osteogenic cells in poly(d,l-lactic-co-glycolic acid)/hydroxyapatite composite scaffolds. *Biomaterials* **29**, 1043, 2008.
194. Costa-Pinto, A.R., Correlo, V.M., Sol, P.C., Bhattacharya, M., Charbord, P., Delorme, B., Reis, R.L., and Neves, N.M. Osteogenic differentiation of human bone marrow mesenchymal stem cells seeded on melt based chitosan scaffolds for bone tissue engineering applications. *Biomacromolecules* **10**, 2067, 2009.
195. Jin, Q.M., Takita, H., Kohgo, T., Atsumi, K., Itoh, H., and Kuboki, Y. Effects of geometry of hydroxyapatite as a cell substratum in BMP-induced ectopic bone formation. *J Biomed Mater Res* **52**, 491, 2000.
196. Yu, H., VandeVord, P.J., Gong, W., Wu, B., Song, Z., Matthew, H.W., Wooley, P.H., and Yang, S.-Y. Promotion of osteogenesis in tissue-engineered bone by pre-seeding endothelial progenitor cells-derived endothelial cells. *J Orthop Res* **26**, 1147, 2008.

Address correspondence to:

Ali Khademhosseini, Ph.D.

Harvard-MIT Division of Health Sciences and Technology  
Massachusetts Institute of Technology  
Cambridge, MA 02139

E-mail: alik@rics.bwh.harvard.edu

Yunzhi Yang, Ph.D.

Department of Orthopedic Surgery  
Stanford University  
Stanford, CA 94305

E-mail: ypyang@stanford.edu

Received: January 11, 2012

Accepted: April 18, 2012

Online Publication Date: September 4, 2012